Escola de Camins
Escola Tècnica Superior d'Enginyeria de Camins, Canals i Ports
UPC BARCELONATECH

TESI DE MÀSTER

Master

MÀSTER UNIVERSITARI EN ENGINYERIA DE CAMINS, CANALS I PORTS

Títol

Numerical modelling of reinforced concrete columns under cyclic loading

Autor

Moldoveanu Andrei

Tutors

JESÚS MIGUEL BAIRÁN GARCÍA

DENISE CARINA SANTOS FERREIRA

Departament

ENGINYERIA DE LA CONSTRUCCIÓ

Intensificació

ESTRUCTURES

Data

Julio 2015

Table of Contents

Table of figures

Abstract

The structural response of reinforced concrete (RC) columns under cyclic loading is investigated. RC elements are presenting very important nonlinearities and in order to be simulated correctly under monotonic and cyclic loading it is essential to account for the nonlinear material phenomena. With this purpose, a state of the art review about the study of the phenomenology and the numerical approaches available to analyze this problem was performed.

In this work is presented a constitutive model for reinforcing steel accounting for the Bauschinger and buckling effects, which are important phenomena that need to be considered in nonlinear cyclic analysis of RC columns. This thesis was centered on the development of an algorithm for the constitutive law of steel. Validation was performed by comparing numerical results with experiments made on bare bars of steel under cyclic loading, available in literature. Afterwards this new algorithm was implemented into an existing FE code CONSHEAR based on the fiber beam formulation with enhanced capabilities regarding accounting for shear effects in the nonlinear response of RC structures. From the preliminary set of examples made to verify the implementation into the FE code, the results are very promising, being able to represent Bauschinger effects in cyclic analysis

Keywords: nonlinear analysis, RC columns, cyclic loading, Bauschinger and buckling effects, Stress - strain relations

1 Introduction

1.1 Problem statement

Studying the structural response of reinforced concrete (RC) columns under cyclic loading is an important topic in the field of structural analysis, both in the assessment of existing structures and also in the design of new ones. Numerical modelling of reinforced concrete elements under cyclic loading includes several specific problems. One of them is the computational time and modelling difficulties brought by the very high nonlinearities present in the problem. In the case of real structures, using solid finite element models can be very complex and time-consuming; hence, its use is usually limited to research and academia environments. In alternative, beam models, as the one used in this work, can be a good alternative in terms of computational and modelling cost, to be applied to the analysis of real structures.

Shear effects, that are traditionally not included in the beam models, can be relevant in the analysis of RC columns submitted to cyclic loading. These elements can be shear critical and failing in a brittle manner due to high shear stresses. Also the interaction of transversal and normal forces can lead to important increments of strains and stresses in concrete and steel; and consequently should not be ignored. Flexural response in reinforced concrete is considered 'solved' in the state-of-the-art. In contrast, shear resistant mechanisms and nonlinear response after diagonal cracking and distribution of forces is still under discussion and many research efforts have been dedicated to this topic in the last years.

A shear-sensitive fibre beam model developed before at UPC (CONSHEAR) was used as the basis of this work. CONSHEAR is a computer program developed for the nonlinear, time-dependent and phased analysis of RC structures accounting for the interaction between axial force, bending and shear force. It has been deeply validated for structures under monotonic loading with shear problems. This work aims to enlarge the application of the model to cyclic analysis of columns. For this purpose it is needed to include a new constitutive law for steel that takes into account the Bauschinger effects.

Buckling of longitudinal reinforcement is also a frequent problem found in RC structures under seismic loading. Hence it is also important to include it in the numerical analysis. The algorithm developed in this work also included this effect.

1.2 Objectives

The main objective of this work is to enhance an existing fibre beam model to make it suitable to perform cyclic analysis of RC columns. In order to achieve this general goal, the following specific objectives were set:

- Study the specific scientific literature on the topic of cyclic loading of RC columns, both in terms of experimental behavior and numerical modelling techniques, to get to know the current state-of-the-art in the field.
- Learn the fundamentals of the background theory and usage of the computer program CONSHEAR.
- Study the Bauschinger and buckling effects of the longitudinal reinforcement.
- Develop an algorithm for a constitutive law for steel that includes Bauschinger and buckling effects, in a manner which can be directly inserted into a nonlinear FE code.
- Validate this constitutive law by comparing numerical results with experiments made on bare bars of steel under cyclic loading, available in literature.
- Insert and link the new constitutive model for steel into the existing FE code CONSHEAR.
- Verify the correct implementation of the new subroutine by running small tests.
- Preliminary validation of the model with experimental tests available in literature of RC columns under cyclic loading by comparing the numerical results with the experimental data.

1.3 Structure of the thesis

The present thesis is divided into 6 chapters:

- Chapter 1 is the present introduction.
- Chapter 2 describes the state of the art focusing on the study of the phenomenology of the structural behavior of RC columns under cyclic loading and the numerical approaches available to analyze this problem. It also highlights the importance of accounting for the shear effects in the numerical studies.
- Chapter 3 resumes the fundamental theory of the numerical model used as basis of this work (CONSHEAR), regarding the different levels of approach of the FEM code: structural scheme, finite element formulation, sectional level approach including multiaxial stress interaction,

constitutive models and treatment of cracking in concrete and procedures for nonlinear analysis. It also states briefly the main modifications done to include the new model for steel.

- Chapter 4 describes in detail the background theory and the development of the algorithm for the new constitutive model for steel including Bauschinger and buckling effects. It also presents the validation of this model against experimental results available in literature of steel bars under cyclic loading. Finally it presents the implementation of the new algorithm in to the basis FE code.
- Chapter 5 presents the verification of the model CONSHEAR with the new constitutive algorithm for steel.
- Chapter 6 points out the main conclusions of this work and sets the possible lines for future developments.

2 State of the art

2.1 Reinforced concrete columns under cycling loading

The reinforced concrete (RC) structure is one of the most widely used earthquake-resistant structural systems in the world. Therefore, extensive research has been conducted on understanding the inelastic cyclic behavior of RC structures under different loading conditions. As a result of these studies, design codes and provisions have been developed and significant improvements in the design practice have been achieved. However, due to the complicated nature of the mechanical behavior, there are still many facets of the response that are not fully understood. The complexity of the problem as many different sources , such as cracking of concrete and nonlinear response, yielding of reinforcing, path dependent responses, interaction of forces, etc.; phenomena that must be accounted in the numerical simulations in order to attain accurate structural analysis.

In the last century, the seismic design of structures has grown from virtually ignored to established requirements and recommendations to predict the earthquake and dynamic behavior of structure, designing the structure, detailing the elements and include energy dissipating devices. Designing frame structures for a lateral level or resistance which can assure an elastic response under design earthquake is not practical by economic and technical point of view. Hence, inelastic response should be considered in these type of analysis.

A resistance level on lateral loads lower than the one needed for the elastic response, results that, even on earthquakes with lower intensity than the design earthquake, the structures mobilize the entire resistant capacity and deform with plastic incursions. This may not mean the breakdown of the building; actually the structural performance under earthquake actions depends on the lateral deformation capacity of the structure. Therefore, the lateral resistant level of a structure depends on its capacity to absorb plastic deformations, without loss of resistant capacity.

It can be observed that any structure made from a material with a nonlinear response (Reinforced Concrete) will start to deform plastically at a certain level of lateral forces. Not all the buildings can absorb plastic deformations while maintaining an acceptable level of lateral resistance. If the nonlinear cyclic deformations are accompanied by a sharp decrease of resistance and lateral rigidity then the capacity to dissipate seismic energy of the building is low and the structure is classified as inductile.

Usually the reinforced concrete structures are seen as structures with good plastic deformations. Therefore, the reduction factor (q) utilized in expressing the design seismic force has high values.

Usually it is admitted to design these type of structures at values of design seismic force of 6-7 times lower than the forces which would ensure an elastic response at design earthquake action.

Yet the simple fact of using a low level of seismic design forces does not guarantee a good ductile response of the structure (even though the plastic deformations are formed). The designer must consider measures to ensure ductility of the structure. A first step is considering an optimum plastification mechanism which could lead to a sufficient earthquake energy dissipation capacity.

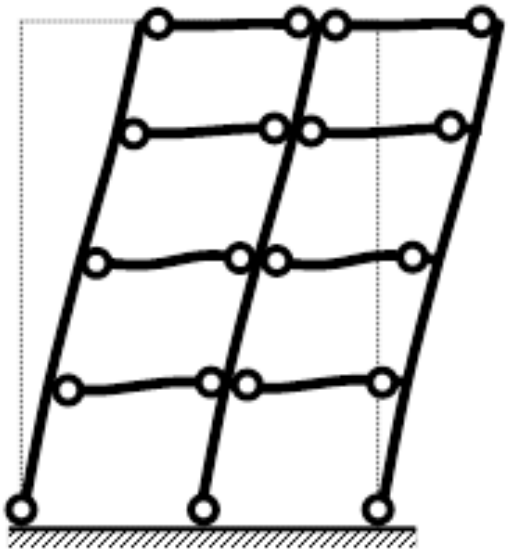

Figure 1 Example of plastification mechanism [1]

Reinforce concrete columns are a common structural solution and maintenance of their integrity in earthquakes is essential to achieve a good building performance in a seismic event. However, analytical estimation of structural response presents difficulties because of the complexity mechanics of component materials. Therefore, evaluation of the seismic behavior of reinforced concrete structures requires conducting experiments.

The seismic response of reinforced concrete columns has been extensively studied with experiments submitted to unidirectional lateral loads. Some of the investigated parameters are: type of cross-sectional geometrical relationship, the axial loading levels, the quantities of the longitudinal and transverse reinforcement, the material supply equipment, among others. A relevant work on this field was developed by Edison 2012 [2], presenting a data base of experimental tests with reinforce concrete columns under bidirectional cyclic loading . He also conducted tests on RC columns under unidirectional and bidirectional cyclic loading and investigated the failure modes [2].

2.2 Numerical nonlinear modelling

RC elements present very important nonlinearities in the structural behavior. In order to simulate correctly RC elements under monotonic and cyclic loading, it is essential to account for the nonlinear material phenomena. Solutions of nonlinear problems, which are prevalent in structural and continuum mechanics, are not of straightforward resolution and, hence, need specific solution techniques. Concrete is a brittle material, presenting cracking brought by different sources of damage, which numerical modelling is not simple.

One single nonlinear solution method may not be capable of solving any general nonlinear problem. Depending on the problem and the severity of the nonlinearities, modifications to solution algorithms are necessary to recover the entire equilibrium path. In an early work, Bergan et al. [3] stated:

"a computer program for nonlinear analysis should possess several alternative algorithms for the solution of the nonlinear system. These procedures should also allow for the possibility of an extensive control over the solution process by parameters that are input to the program. Such a scheme would lead to increased flexibility, and the experienced user has the possibility of obtaining improved reliability and efficiency for the solution of a particular problem."

Many authors have developed families of nonlinear solution schemes, which can be adjusted by the user depending on the problem. Mondkar and Powell [4] developed a library of algorithms based on the Newton-Raphson method. Seven solution schemes were formulated from 11 control parameters (stiffness update type and frequency, convergence tolerance, etc.) and tested on several nonlinear structural systems. Clarke and Hancock [5] used the concept of load increment from the standard or modified Newton-Raphson method to unify several nonlinear solution schemes through a single load factor. The specific incremental iterative procedure depends on the chosen constraint equation, which is used to calculate the unifying load factor. The constraint equations are based on iterations at constant load, displacement, work, arc length, or minimum residual. Yang and Sheih [6] presented a similar library of nonlinear solvers unified through a single load parameter, and included the generalized displacement control method. More recently Rezaiee-Pajand et al. [7] unified five nonlinear solution schemes through a single general constraint equation. The schemes were identified by five different constraints, including minimizing error by means of its length, area, or perimeter, and then the strengths and weaknesses of each algorithm were evaluated.

The most versatile approach is the analysis of spatial reinforced concrete structures by means of solid finite elements (FE), however, this technique can be very computationally complex, when applied to nonlinear analysis of structures involving multiple members and complex loading schemes. Beam 1D (linear) elements can be preferred as an economical alternative for practical usage and to be applied at true structural scale with affordable computation and modelling times.

Several beam element models suitable for the analysis of reinforced concrete structures have been proposed to date presenting different strategies for treatment of nonlinearities:

- Concentrated plasticity methods are based on the fact that the nonlinear behavior of reinforced concrete framed structures is generally concentrated at the end of columns and girders. These methods concentrate the inelastic behavior in nonlinear springs located at the ends of the elements (Figure 2). Examples of these methods were proposed by Clough and Jhonston (1966 [8]), Giberson (1967 [9]), and Takizawa (1976 [10]), among others. Some of these methods include stiffness degradation in flexure and shear (Clough and Benuska 1967 [11], Takeda et al. 1970 [12], Brancaleoni et al. 1983 [13]), "pinching" under reversal load (Banon et al. 1981 [14], Brancaleoni et al. 1983 [13]) and fixed-end rotations at the beam-column joint interface to simulate the effect of bar "pull-out" (Filippou and Issa 1988 [15]). Filippou and Issa 1988 [15] applied his model to cyclic analysis.

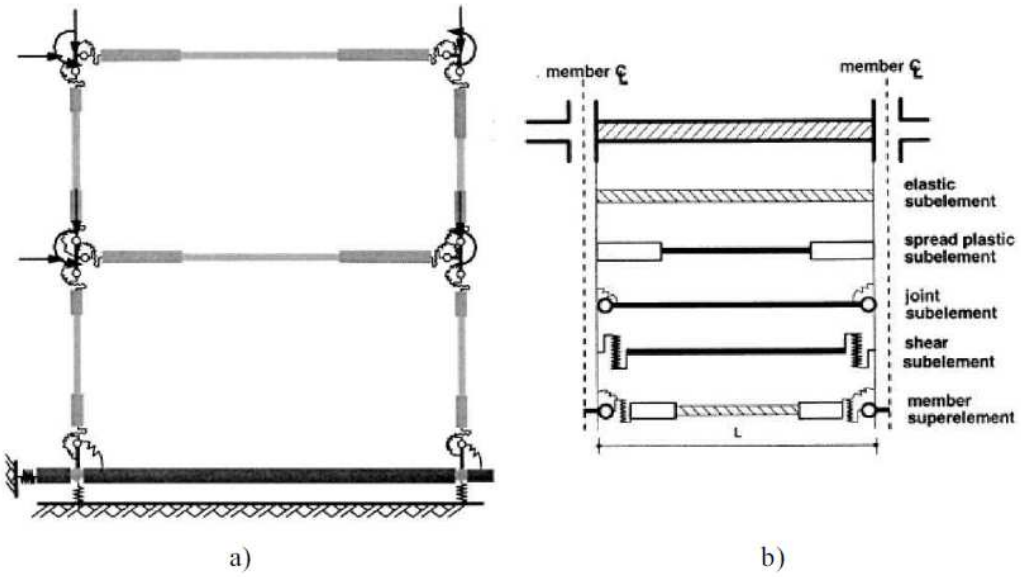

Figure 2 Typical concentrated plasticity model a) Two story frame model b) Typical frame element (Filippou et all. [16])

- Distributed nonlinearity methods are a more accurate approach for the modelization of the inelastic behavior of reinforced concrete structures, consisting of distributing the nonlinearity along the length of the members. The constitutive behavior of the cross section is either formulated in terms of stress and strain resultants derived from the classical plasticity theory or is explicitly derived by the discretization of the cross section into fibers. In a fiber finite element model, the member is discretized both longitudinally, into segments represented by discrete cross-sections or slices, and at the cross sectional level, into finite regions. In the more general case of biaxial bending, the cross-section is divided into a number of finite regions by a rectangular grid of lines. These formulations have been successfully employed in the nonlinear analysis of reinforced concrete framed structures, as in Buckle and Jackson (1981 [17]), Mahasuverachai and Powell (1982 [18]), Kaba and Mahin (1984 [19]), Chan (1981 [20]), Mari (1984 [21]), Ulm et al. (1994 [22]), Petrangeli and Ciampi (1997 [23]) or Spacone et al. (1996 [24]), among others. Petrangeli and Ciampi (1997 [23]) or Spacone et al. (1996 [24]) applied the models to the study of RC elements under cyclic loading.

- Distributed nonlinearity methods including shear: Saritas and Filippou (2006 [25]) and Petrangeli et al. (1999 [26]) proposed fiber element models for cyclic analysis of reinforced concrete structures including bending and shear. More recently, Bairán and Mari (2007 [27]) developed a nonlinear sectional formulation to account for full 3D stress-strain states on frame elements (TINSA). This approach is applied to the nonlinear coupled behavior of reinforced concrete sections and may be implemented on any 3D frame element without introducing additional degrees of freedom on the frame element. Mohr (2010) [28] passed the TINSA model to the element level and performed cyclic analysis with beam elements including shear.

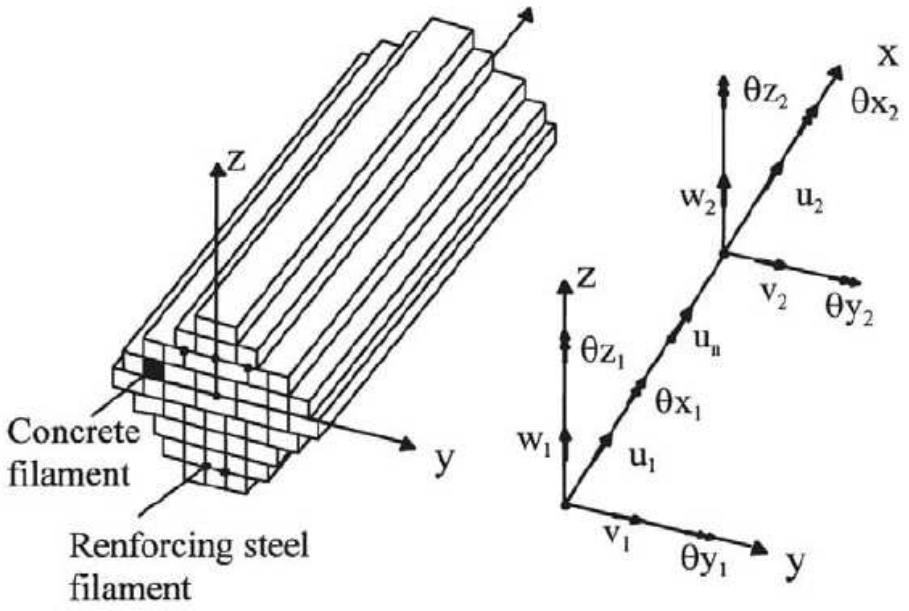

Figure 3 Typical filament beam element model (Mari 2000 [29])

Two different approaches are used in the derivation of the member stiffness: the stiffness approach where the nodal displacements of the structure are derived from the element forces, and the flexibility approach, which considers the member forces as the primary unknowns. The second one permits a more accurate description of the force and stress distribution inside the member.

An alternative for the nonlinear analysis of frame structures, which provides a virtually "exact" solution, is the so-called Generalized Matrix Formulation (GMF). This approach is a forced-based formulation which means that internal forces are interpolated along the element length instead of displacements, as in the traditional displacement-based (stiffness) approach (FEM). In this manner GMF elements automatically consider shear deformations but are not based on Timoshenko's beam theory. This approach was used by Carrascon et all (1987 [30]), Carol and Murcia (1989 [31]), Mari (1991 [32]) among others.

The material models in static nonlinear analysis requires the description of cyclic behavior when redistribution takes place because it provokes new loading, unloading and reloading in the materials.

2.2.1 Uniaxial cyclic concrete modelling

The concrete constitutive laws are different for tension and compression. The behavior in each range is often described with stress - strain backbone curve. A common assumption is that the envelope curve for concrete subjected to axial cyclic compression can be approximated by the monotonic stress-strain curve.

The cyclic behavior of concrete is complex and significant research effort has been made in the last decades resulting into numerous concrete models . In the macroscopic level, three broad categories can be distinguished (CEB 1996 [33]): models derived from the theory of elasticity; models based on the theory of plasticity; and, models based on the continuum damage theory. Also, some coupled models based on the association of plasticity and continuum damage theory have been recently developed. A summary of existing models and a new approach is presented in (Sima 2010 [34])

(Karsan and Jirsa 1969 [35]) carried out an experimental work that led to the results presented in Figure 4. It shows the stress-strain diagram of a concrete cylinder subjected to repeated uniaxial compression involving loading and unloading under deformation control.

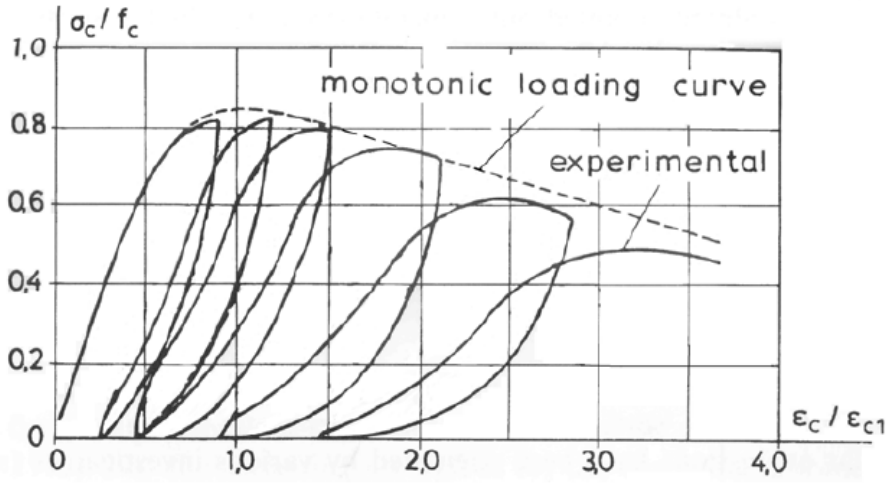

Figure 4 Cyclic uniaxial compression with full unloading (Karsan and Jirsa 1969 [35]*)*

A total of 46 short rectangular columns were tested under cyclic varying axial loads. This work was carried out with the goal of determining the stress-strain envelope and the unloading and reloading curves. The experimental results indicated that the stress-strain paths under cyclic loading generally do not exceed the envelope curve; furthermore, this curve can be modeled as the stress-strain curve obtained under monotonic loading to failure.

When reloading starts from zero stress to meet the envelope curve, it is found that the reloading curve becomes rather flat in most of its range and may be represented by a simple straight line (Sinha et all.1964 [36]) or a second-order parabola (Karsan and Jirsa, 1969 [35]).

2.2.2 Uniaxial Steel model

The behavior of the reinforcing steel is an important issue which may have a great influence in the overall response of reinforced concrete (RC) members under cyclic or dynamic loadings. When subjected to seismic excitation, reinforcing bars inside RC structures experience wide range of strain variations (large tensile and compressive strains) and also random strain reversal from different strain levels. To overcome the previous mentioned necessities a reliable path-dependent cyclic stress-strain relationship which can cover all possible strain paths is necessary for evaluating structural seismic performance analytically.

When subjected to cyclic loading, steel exhibits a loss of linearity prior to the attainment of the yield strength in the opposite direction. This characteristic, known as Bauschinger effect, has been observed that becomes more pronounced when increasing the strain demand (Ma et all [37]). Several models for the reinforcing steel accounting for the Bauschinger effect and other characteristics of the steel behavior have been proposed to date (Mander et all 1984 [38], Dodd and Posada 1995 [39] ,Filippou et all 1983 [40]). However they do not include the effect of buckling and their applicability is limited to thick bars that are unlikely to buckle within reasonable compressive strain range or to loading cases where strain does not reach high levels in compression.

Because buckling of reinforcing bars in RC member is a common phenomenon during seismic excitations, a proper model that takes this into account is needed. Buckling induced instability of reinforced bars in RC members has been studied by Zigone et all 1988 [41], Mau and Mounir 1989 [42], Watson et all 1994 [43]. These proposals don't include cyclic response.

Complete cyclic models that include effect of buckling have been proposed by Monti and Nuti 1992 [44] Pantazopoulou 1998 [45], Suda et all 1996 [46], Rodriguez et all 1999 [47], Dhakal and Maekawa 2002 [48], Stanton et all. 2006 [49].

For cyclic loading Giuffre-Menegotto-Pinto proposed a model for reinforcing steel subjected to load reversal .This model was initially proposed by Giuffre and Pinto [50] and later used by Menegotto and Pinto [51]. The loading and unloading paths are contained in a bilinear envelope. Their equations where improved by Filippou et all [40]. A more detailed description of the model is given in Chapter 3.2 as it is the model implemented in this work.

2.2.3 Shear effects

Shear effects may be relevant in the analysis of RC elements under cyclic loading. Shear failures are brittle and are the most observed failure modes in the recent earthquakes. However, in contrast with bending mechanisms, shear resistance in RC is still a matter under discussion among various researchers worldwide. When performing a numerical analysis of RC elements under cyclic loading it is essential to account for the effects of shear; because shear can be the critical failure mode and also because it interacts with other forces and influences the structural behavior. This is even more important in the assessment of existing structures, that may be critical to shear, due to less conservative earlier codes regarding shear.

Relevant models for RC under cyclic loading including shear effects were developed in the past:

- Petrangeli et all. (1999 [26]) developed a microplane model based on a kinematic constraint relating the external stains with those on selected internal planes and on the monitoring of simple stress-strain relationships on these planes. The authors proposed a flexibility-based fiber beam element for modeling the shear behavior and its interaction with axial force and bending moment in RC beams and columns, which leaded to a 2D element with two nodes. The fiber element was implemented in the code program *E.F.FIBRE* (Petrangeli and Ciampi, 1994 [52]).

- Kotronis et all. (2005 [53]) presented a fiber beam column using a damage model. The authors proposed a 3D multifiber beam element capable of taking into account of shear response according to the Timoshenko theory. It was used a series of Lagrangian polynomials for the interpolation of transverse and rotational displacements. The proposed model was implemented in the library FEDEAS (Filippou and Spacone 1996 [54]) of the finite element code FEAP (Taylor 2000 [55])

- Mohr (2010 [28]) proposed a shear-sensitive model based on GMF approach that computes shear strains as a series of polynomials. It accounts for the nonlinear interaction between shear and normal forces and allows for cyclic loading analysis.

This work represents a preliminary extension of an existent FEM based on the fiber beam approach accounting for force interaction (bending, shear and axial force) to the cases of cyclic loading. Fibre beam models with shear effects may be advantageous for real scale assessment of structures. To do this, the basic model has to include new features, such as, the effects of cyclic loading in the material models and enhanced solutions for the nonlinear problem. The advantage of CONSHEAR is related with the fact of being a relatively simple model, accounting for shear effects, and with possibilities of being used in practice.

3 Numerical model

3.1 Overview

CONSHEAR (Ferreira 2013 [56]) is a computer program for the nonlinear analysis of reinforced and prestressed concrete frame structures by means of the fiber beam element approach and accounting for axial force-shear-bending interaction. The numerical model implemented in CONSHEAR is based on a previous model founded on the Finite Element Method (FEM) and on the Bernoulli's beam theory that is implemented in the computer program CONS (Marí 1984 [21]; Marí 2000 [29]).

CONSHEAR is an upgrade version of model CONS by broaden its applications to analysis including shear. In general, its main characteristics are: the Timoshenko beam theory is assumed at the element level; a hybrid sectional formulation, in which input variables comprises both kinematical and force quantities, links the plane section theory with the assumption of a constant shear stress flow. The multiaxial constitutive behavior of concrete is assumed through a smeared crack approach with full rotating cracks; compression weakening (softening) and tensile tension stiffening effects are included. Longitudinal reinforcement is simulated through the use of steel filaments while transversal reinforcement is considered smeared in the concrete fibers. The computer algorithm that implements CONSHEAR is written in FORTRAN77 language. It presents a module configuration in a way that can be improved by changing, adding or replacing subroutines in order to consider more aspects of the structural behavior.

3.1.1 Structural Scheme

In numerical simulations by means of the FEM using 1D fiber beam models the structure is divided into elements interconnected by nodes and the material nonlinearities are introduced at each control section that is discretized into longitudinal fibers as observed in Figure 5. The sectional model of CONSHEAR accounts for the axial-shear-bending interaction in a direct manner and also the multiaxial nonlinear response of each concrete fiber. Boundary conditions are reproduced by means of elastic supports (rotation and displacement in each direction). These conditions can vary in time in order to simulate phases of construction. Also variations on the degrees of freedom of the elements allow the consideration of hinges or relative displacements between elements. These restraint conditions may also vary throughout the construction process and the life-time of the structure.

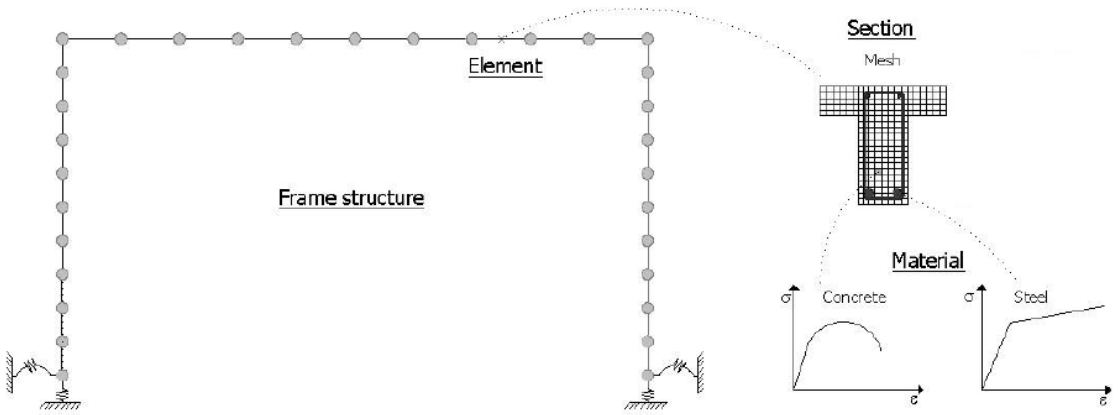

Figure 5 General characteristics of the fiber beam models (Ferreira 2013 [57]*)*

3.1.2 Fundamentals

CONSHEAR is a displacement-based shear-sensitive fiber beam FE model devised for analyses of 3D RC frames under combined axial, bending and shear forces. Axial force shear - bending interaction is only included in the plane level (2D). The general characteristics of the basic model CONSHEAR are:

- beam-type linear Timoshenko FE;
- cross-sections are discretized into fibers (concrete and smeared transversal reinforcement) and filaments of longitudinal reinforcement;
- concrete fibres have multiaxial strain-stress states;
- reinforcement is assumed to be in a 1D strain-stress sate;
- perfect bond between concrete and steel is assumed;
- smeared crack theory assumed for concrete simulation;
- normal-shear forces interaction (N-M-V) at the sectional level is considered in all levels of material damage;
- material and geometric nonlinearities are considered;
- nonlinear analysis is performed within a Newton-Raphson framework.

The model can also be used to time-dependent and phased analysis of concrete structures.

3.1.2.1 Finite element

A 2-noded Timoshenko finite element with linear shape functions is used in the model.

For the 2D case, the displacement field is a function of two displacements, axial *u* and vertical *w*, and a rotation ϑy. In the Timoshenko beam theory it is assumed that undeformed plane sections perpendicular to the beam axis remain plane but not necessarily normal to the longitudinal axis after deformation. An average rotation of the section due to distortion is considered in order to maintain valid the plane section assumption.

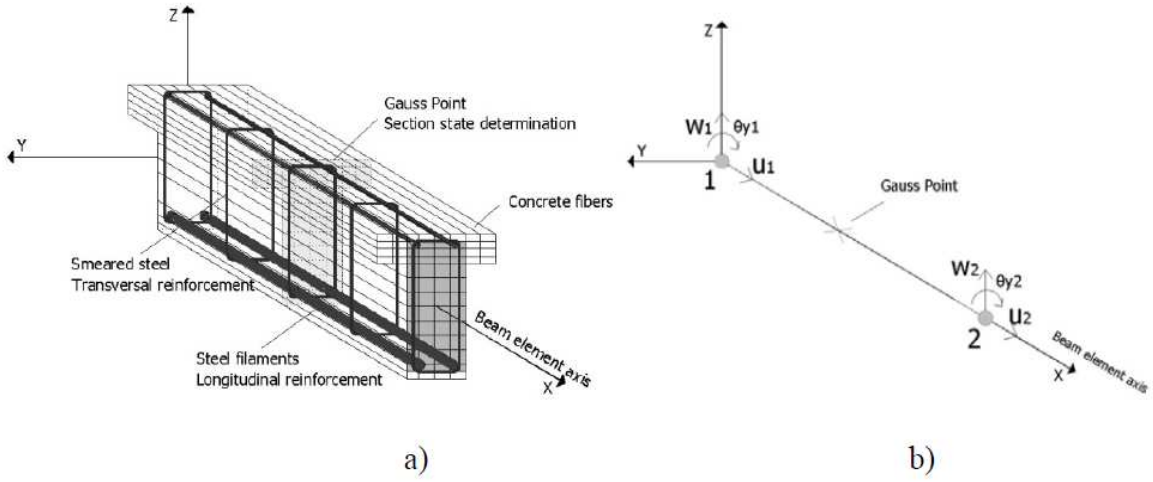

Figure 6 Fiber beam model in CONSHEAR: a) general characteristics b) finite element for the 2D case (Ferreira 2013 [57]*)*

3.1.2.2 Sectional level

RC sections of arbitrary shape are divided into fibers of concrete and smeared transversal reinforcement and filaments of longitudinal reinforcement (Figure 7). Consequently, it is possible to assign different materials to different fibers and filaments in a cross-section.

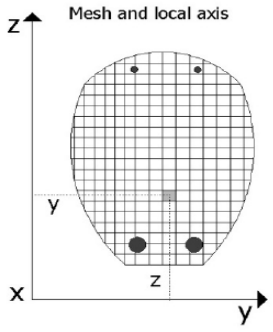

Figure 7 Discretization of the cross section (Ferrerira 2013 [57]*)*

The cross-section is discretized into two types of fibers, as presented in Figure 8:

- non-shear resistant ones, submitted to 1D axial stresses only;
- shear resistant fibers, submitted to a multiaxial stress-strain state.

Axial force and bending moment are resisted by the entire cross-section; shear forces and interaction with normal forces are only considered in the shear resistant fibers.

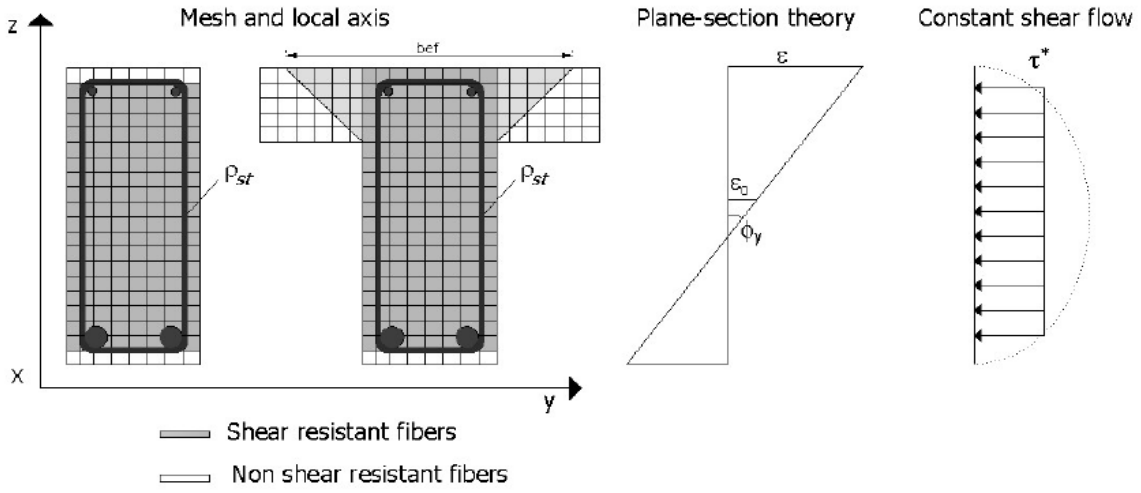

Figure 8 Assumptions of the model at the section level (Ferreira 2013 [57]*)*

This fiber subdivision is an input of the model related to the shape of the cross section: for rectangular, T-shape and I-shape, the fibers that pertain to the web (disregarding the bottom cover area) are considered shear resistant. Particularly for the T-shape and I-shapes cross sections, if there is strong evidence that compressive flanges contribute to the shear-resistance mechanism, an effective area of the flange b_{eff} determined according to (Zararis et all [58]) can be considered as 2D fibers.

The classical equations for the element stiffness matrix, K_{elem}, and the internal resistant load vector, F_{elem}, are written in the following manner, by using sectional model:

$$K_{elem} = \int B\, K_{sec}\, B\, dx$$

$$\underline{F}_{elem} = \int B^T\, \underline{S}_{sec}\, dx$$

These integrals are solved through the Gaussian quadrature method and reduced integration is considered to avoid shear locking (Zienkiewicz and Taylor [59]).

3.1.2.3 Material models

The adopted 2D constitutive law for concrete is based on the Modified Compression Field Theory (MCFT) (Vecchio and Collins [60]), being formulated in terms of average strains $\varepsilon_{12} = [\varepsilon_1\ \varepsilon_2]^T$ and stresses $\sigma_{12} = [\ \sigma_1\ \sigma_2]^T$ between the undamaged and cracked areas. Cracked concrete is assumed as a homogeneous material with orthotropic behavior (Figure 9(a)).

The curve considered for concrete in compression is presented in Figure 9 (b): ε_p is the strain at peak stress f_p and ε_{p2} is the plastic strain after unloading by means of the initial stiffness E_0.

For concrete in tension (Figure 9(c)) a linear response is considered before cracking and remaining stresses in the cracked stage: f_t and ε_{cr} are respectively the maximum tensile stress and strain of concrete for which cracking appears.

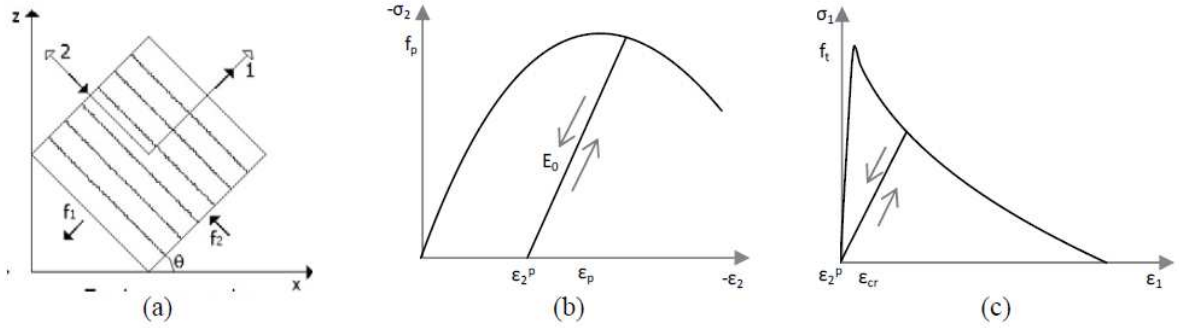

Figure 9 Constitutive model for concrete: a) smeared crack b) compression c) tension [57]

Longitudinal (passive) and transversal (passive or active) reinforcements are considered under 1D stress-strain states by means of a bilinear uniaxial constitutive equation with kinematic hardening (Figure 10): f_{sy} and ε_{sy} correspond to the yielding strength and strain and f_{su} and ε_{su} to the ultimate strength and strain of the reinforcement material (e.g. steel, fibre reinforced polymers – FRP, etc.).

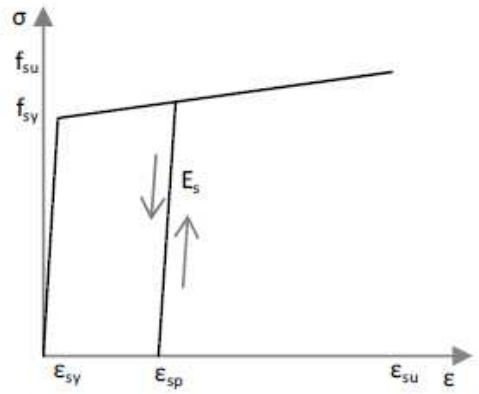

Figure 10 Constitutive model for the reinforcement

3.1.2.4 Procedures for nonlinear analysis

Implementation of the model is illustrated by the flowchart presented in Figure 11, where two iterative loops are marked:

(1) an outermost one, which corresponds to the standard Newton-Raphson procedure for determination of the displacement increments through the global equilibrium equations;

(2) the innermost iteration loop that corresponds to the state determination of the shear resistant fibers.

Considering the outermost iterative procedure a continuation technique, an arc-length based on the Updated Normal Plane (Crisfield [61]) is available.

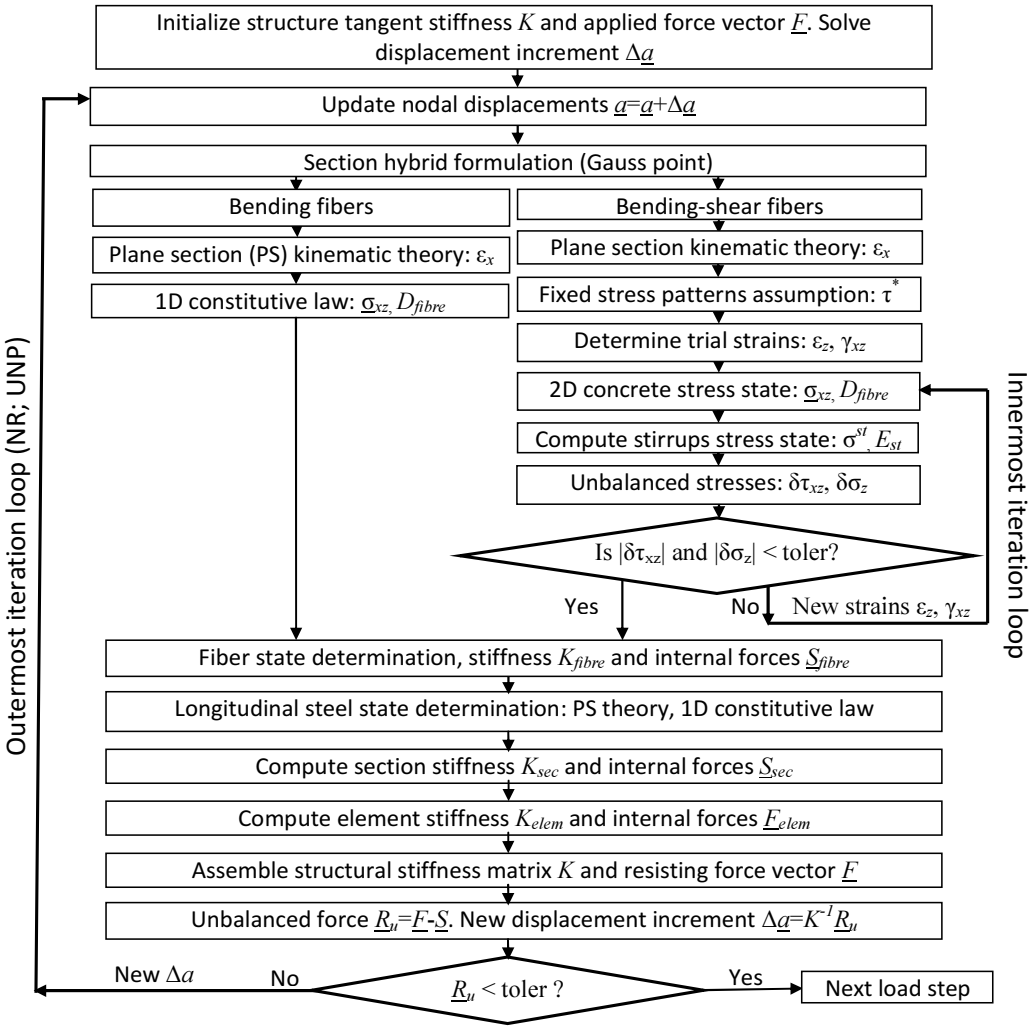

Figure 11 Flow chart of ConShear

3.1.2.5 Modifications in CONSHEAR

The purpose of this work is to improve the steel constitutive model and enhance if with a new path-dependent cyclic stress–strain relationship of reinforcing bar including buckling. It takes into the account the effect of geometrical and mechanical properties of the bar on its post-buckling response which make it applicable to bars with any material properties and any type of hardening mechanism. The formulation is computationally efficient, using $\sigma = f(\varepsilon)$ relation for the loading branches with full path depending which covers all possible strain paths, and is developed in a manner ready to be implemented in any FE code as an independent constitutive law for steel. This model is used for both longitudinally and transversally reinforcements. The algorithm is adapted to Fortran 77 in order to be implemented in CONSHEAR.

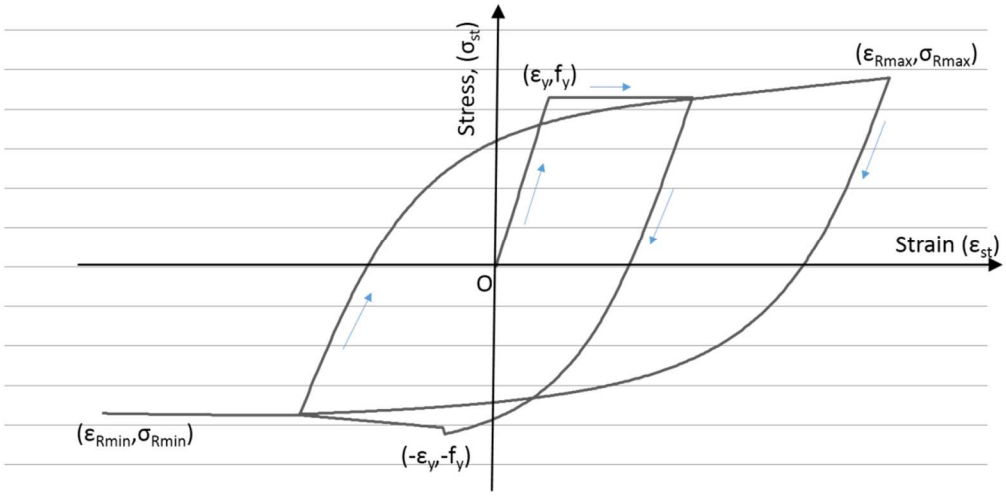

Figure 12 New constitutive model for reinforcement

4 Steel model for cyclic analysis

4.1 Theoretical formulation

Accurate modeling of reinforcing steel stress-strain behavior is important for predicting the response of reinforce concrete structures.

Reinforcing bars inside RC structures experience wide range of strain variations when subjected to a seismic excitation. Apart from experiencing large tensile and compressive strains, these bars also undergo random strain reversals from different strain levels. As the post-elastic response of reinforcing bars depends on the strain history, a reliable path-dependent cyclic stress-strain relationship that can cover all possible strain paths is deemed necessary for evaluating structural seismic performance analytically.

Past earthquakes have shown that a common failure mode of reinforced concrete (RC) members is buckling of the longitudinal reinforcement. In order to obtain an accurate prediction of strength and ductility, this effect should be taken into account during analysis. Buckling of the reinforcement is, in essence, a stability problem and therefore depends both on the geometry of the bar and on the material properties.

The considered model is based on a path-dependent cyclic stress–strain relationship of reinforcing bar including buckling. It takes into account the effect of the geometrical and mechanical properties of the bar on its post-buckling response which makes it applicable to bars with any material properties and any type of hardening mechanism.

The following sections present the detailed description of the theoretical background present in the new model for steel.

4.1.1 Uniaxial monotonic curve

4.1.1.1 Tension envelope

The tension envelope, as shown in Figure 13, consists of four parts:

- an elastic branch (O–Y);
- a yield plateau (Y–H);
- a strain-hardening zone (H–U);
- and the post ultimate descending branch (U–F).

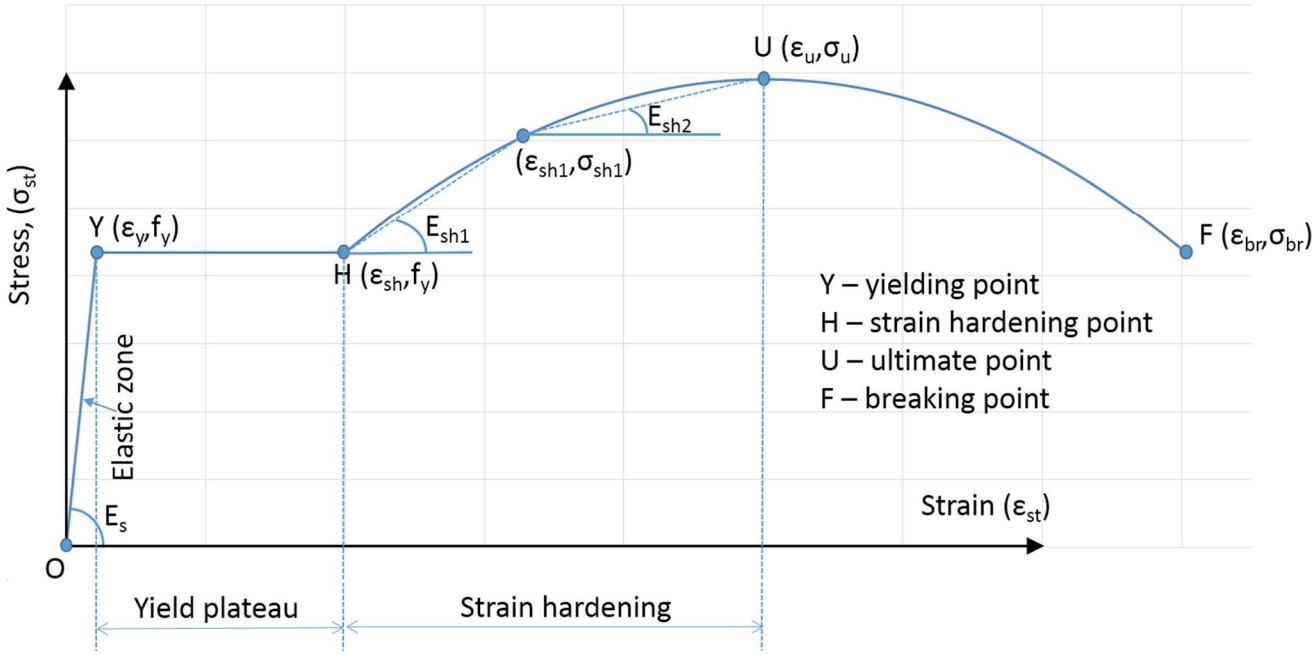

Figure 13 Schematic representation of monotonic tension envelope

Although a closer look inside the yield plateau is reported to reveal small stress undulations [39], for simplicity, it is represented here as a straight line with the stress equal to the yield strength. The tension envelope is considered until the ultimate stress point (ε_u) and can be represented by the following uniaxial stress–strain (σ_{st}-ε_{st}) relationships:

$$\sigma_{st} = E_s \varepsilon_{st} \qquad \text{for } \varepsilon_{st} \le \varepsilon_y \tag{1}$$

$$\sigma_{st} = f_y \qquad \text{for } \varepsilon_y < \varepsilon_{st} \le \varepsilon_{sh} \tag{2}$$

$$\sigma_{st} = f_u + (f_y - f_u)\left(\frac{\varepsilon_u - \varepsilon_{st}}{\varepsilon_u - \varepsilon_{sh}}\right)^P \qquad \text{for } \varepsilon_{sh} < \varepsilon_{st} \le \varepsilon_u \tag{3}$$

in which the variables are represented by the following parameters:

E_s – Young's Modulus;

f_y - yield strength;

ε_y - yield strain;

ε_{sh} - strain at the starting point of hardening;

ε_u - ultimate strain;

f_u – ultimate strength.

P is a parameter that describes the shape of the hardening curve and can be calculated as:

$$P = E_{sh}\left(\frac{\varepsilon_u - \varepsilon_{sh}}{f_u - f_y}\right) \tag{4}$$

where E_{sh} is tangential stiffness of the hardening curve at the starting point;

Note: P=0 (E_{sh}=0) represent an elasto-plastic bar;

P=1 ($E_{sh}=(f_u-f_y)/(\varepsilon_u-\varepsilon_{sh})$) represent a bar with linear strain-hardening behavior.

Because it can be hard to estimate the tangential stiffness (Esh) an alternative solution for calculating P is given by Rodriguez et all [47] which utilizes the coordinates of any point (εsh1, fsh1) in the strain-hardening zone:

$$P = \frac{\log(\frac{f_u - f_{sh1}}{f_u - f_y})}{\log(\frac{\varepsilon_u - \varepsilon_{sh1}}{\varepsilon_u - \varepsilon_{sh}})} \quad (5)$$

However, the selection of the intermediate point (ε_{sh1}, f_{sh1}) is difficult. When only the extreme points of the strain-hardening curve are supplied and the nature of the hardening curve in between is not known, it is recommended to assume:

$$\varepsilon_{sh1} = \left[0.5(\varepsilon_{sh} + \varepsilon_u)\right] \quad (6)$$

$$f_{sh1} = \left[f_y + 0.75(f_u - f_y)\right] \quad (7)$$

4.1.1.2 Compression envelope

The model for compression envelope used in this work was proposed by Maekawa and Dhakal [62]. Through this analytical parametric study, various issues regarding the average behavior of reinforcing bars in compression are discussed, such as:

- The average compressive stress-strain relationship can be completely described by $L/D\sqrt{fy}$;
- The average compression envelope lies below the tension envelope when plotted together;
- The trend of average compressive stress degradation depends on the value of $L/D\sqrt{fy}$ and also on the tension envelope;
- Regardless of $L/D\sqrt{fy}$, the compressive stress degradation rate in the later stage is nearly constant with a negative slope approximately equal to $0.02E_s$;
- The average compressive stress becomes constant after it becomes equal to 20% of the yield strength.

Guided by these unique interrelationships, an average monotonic compressive stress-strain relationship was proposed; the general layout is sketched in Figure 14. Note that the compressive stresses and strains specified in Figure 14 and used in the equations to follow are absolute, and their signs should be changed before merging with the tension envelope and unloading/reloading loops to

form a complete cyclic model. An intermediate point *(ε_i, fi)* is established, after which a constant negative stiffness equal to $0.02E_s$ is applied until the average compressive stress becomes equal to $0.2f_y$.

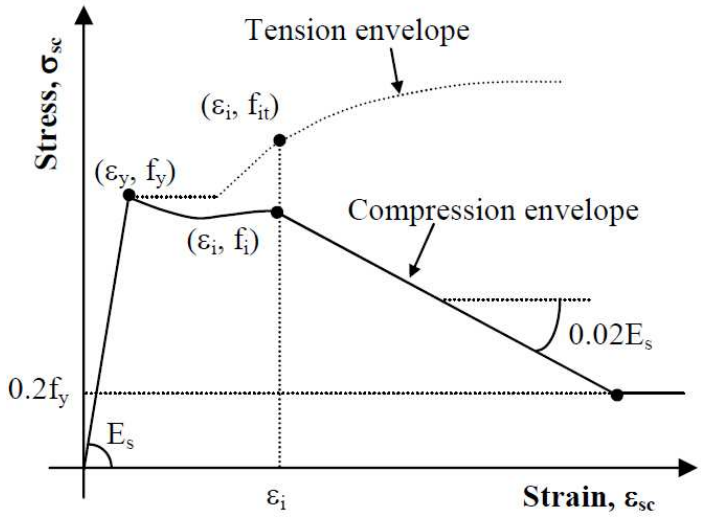

Figure 14 Schematic representation of proposed model[48]

The following compressive stress-strain (σ_{st}-ε_{st}) relationships are proposed:

$$\sigma_{sc} = E_s \varepsilon_{sc} \qquad \text{for } \varepsilon_{sc} \le \varepsilon_y \tag{8}$$

$$\frac{\sigma_{sc}}{\sigma_t} = 1 - (1 - \frac{f_i}{f_{it}})(\frac{\varepsilon_{sc} - \varepsilon_y}{\varepsilon_i - \varepsilon_y}) \qquad \text{for } \varepsilon_y < \varepsilon_{sc} \le \varepsilon_i \tag{9}$$

$$\sigma_{sc} = f_i - 0.02E_s(\varepsilon_{sc} - \varepsilon_i) \qquad \sigma_{sc} \ge 0.2f_y \qquad \text{for } \varepsilon_{sc} > \varepsilon_i \tag{10}$$

in which:

ε_{sc} is the current strain;

ε_i is the strain at the intermediate point;

σ_t ,f_{it} is the stresses in the tension envelope corresponding to ε_{sc}.

To make the model applicable to bars made with all types of material model, the compressive stress (σ_{sc}) at and before the intermediate point is normalized with respect to σ_t. This normalization technique also renders the shape of the average compression envelope before this intermediate point look like the tension envelope; a characteristic that was distinctly observed in all analytical results. The coordinates of intermediate points in the analytically generated average compression envelopes could be correlated to $L/D\sqrt{fy}$ as:

$$\frac{\varepsilon_i}{\varepsilon_y} = 55 - 2.3\sqrt{\frac{f_y}{100}}\frac{L}{D} \quad \frac{\varepsilon_i}{\varepsilon_y} \geq 7 \tag{11}$$

$$\frac{f_i}{f_{it}} = \alpha(1.1 - 0.016\sqrt{\frac{f_y}{100}}\frac{L}{D}) \quad \frac{f_i}{f_{it}} \geq 0.2 \tag{12}$$

Comparison between the average compression envelopes of the elastic perfectly plastic and the linear strain hardening bars revealed that, the normalized strain at the intermediate point ($\varepsilon_i/\varepsilon_y$) was almost unaffected, but the normalized stress (f_i/f_{it}) was sensitive to the nature of strain hardening. To account for this effect, a coefficient α is included in the formulation of stress at the intermediate point in equation (12).

The value of α *is*:

- 0.75 for elastic perfectly plastic bars
- 1 for bars with continuous linear hardening

For bars with limited hardening range, which in the case of most of the industrial products, the value parameter it should be chosen between 0.75 and 1. If the hardening stiffness is very small or the hardening range in terms of strain is short, α should be closer to 0.75. On the other hand, if the hardening lasts for large strain range, it should be closer to 1.0. To represent this qualitative interrelationship, the following equations are recommended to compute α*:*

$$\alpha = 0.75 + \frac{\varepsilon_u - \varepsilon_{sh}}{300\varepsilon_y} \quad \text{limited to } \alpha \leq \frac{f_u}{1.5f_y} \quad \text{limited to } 0.75 \leq \alpha \leq 1.0 \tag{13}$$

4.1.2 Uniaxial cyclic loops including Bauschinger effect

The Bauschinger effect refers to a property of materials where the strain-stress characteristics change as a result of the microscopic stress distribution of the material. It is normally associated with conditions where the yield strength of a metal decreases when the direction of strain is changed. This influences energy dissipation, and both ductility and strength of the structure when submitted to cyclic loadings.

Tangential stiffness of compression envelope that includes buckling may not always be positive, and the possible negative stiffness varies widely depending on the geometrical and mechanical properties of the bar. A negative stiffness at the minimum strain point may generate an unloading curve that shows compressive stress reduction even before entering the compressive strain zone. This tendency in the cyclic loops can be simulated only if the stiffness at the target point is also taken into account in formulating the trajectory of the loop. Therefore, Giuffre–Menegotto-Pinto model [51] that satisfies the aforementioned condition is adopted in this study, and some modifications are made to account for the effects of buckling.

The Giuffre-Menegotto-Pinto model was initially proposed by Giuffre and Pinto [50] and later used by Menegotto and Pinto [51]. The loading and unloading paths are contained in a bilinear envelope defined by:

$$\sigma^* = b\varepsilon^* + \frac{(1-b)\varepsilon^*}{(1+\varepsilon^{*R})^{1/R}} \tag{14}$$

where b is strain-hardening ratio defined by the ratio between the intended slope at the target point (E_1) and the unloading/reloading stiffness at the origin (E_s):

$$b = \frac{E_1}{E_s} \tag{15}$$

The normalized stress and strain ε* and σ* are obtained by a variable substitution. Their equations where improved by Filippou et all [40] :

$$\varepsilon^* = \frac{\varepsilon - \varepsilon_R}{\varepsilon_{Int} - \varepsilon_R} \tag{16}$$

$$\sigma^* = \frac{\sigma - \sigma_R}{\sigma_{Int} - \sigma_R} \Rightarrow \sigma = \sigma^*(\sigma_{\text{int}} - \sigma_R) + \sigma_R \tag{17}$$

where ε_R,σ_R are the strain and stress where the last load reversal occurred (point A in Figure 15) and ε_{int},σ_{int} represent the intersection (point Int. in Figure 15) of the two tangents.

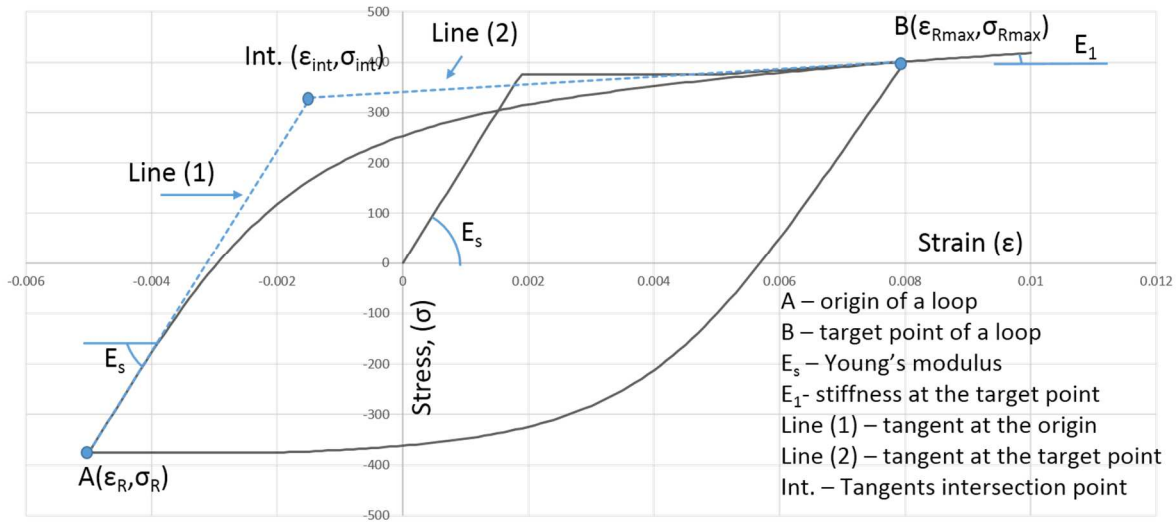

Figure 15 Menegotto-Pinto steel model

The distance to the elastic curve, which simulates the Bauschinger effect, is a function of the parameter R defined by:

$$R = R_0 - \frac{a_1 \xi}{a_2 + \xi} \tag{18}$$

where: R_0, a_1 and a_2 are material constants and ξ is the absolute value of the plastic strain of the last excursion .

In ref [34] ξ is computed as:

$$\xi = \frac{\varepsilon_{R\max} - \varepsilon_0}{\varepsilon_0 - \varepsilon_R} \tag{19}$$

This formulation is convenient because it requires only one parameter to store and update (maximum reload point in tension and compression - ε_{Rmax}).

In the model the following parameter values are used:

$R_0 = 20$

$a_1 = 18.5$

$a_2 = 0.15$

Note that the target point always lies in an envelope although the origin can be inside a loop itself. As the maximum and minimum strain points are target points for potential cyclic loops, the stiffness at these extreme points is also stored in the memory in addition to their coordinates. These values are updated once the strain goes outside the range defined by the positive and negative maximum strains. To ensure path-dependency, a new tangent intersection point is established and the value of R is computed for each new strain reversal.

In order to account for the effects of random loading, a set of rules is introduced, extending the validity of the model, although limiting the amount of memory required to keep into account the past stress-strain history. As proposed by Filippou et all [40], only four controlling curves are memorized and considered at each step:

- The monotonic envelope;
- The ascending upper branch curve, originating at the reversal point with the smallest ε value;
- The descending lower branch curve, originating at the reversal point with the largest ε value;
- The current curve, originating at the most recent reversal point.

4.1.3 Stiffness at target and origin point

For a reloading loop as shown in Figure 15, the target point is the maximum tensile strain point, and the target stiffness is equal to the hardening stiffness at the maximum strain point stored in the memory.

For an unloading loop, the tangential stiffness at the target point (maximum compressive strain ever reached) can be positive or negative depending on the extent of buckling occurred before. The target stiffness, if positive, is always smaller than the tangential stiffness of the tension envelope at an equal tensile strain. On the other hand, depending on the value of the parameter $L/D\sqrt{fy}$, the negative tangential stiffness varies widely. Using a large negative value for the target stiffness is likely to generate unloading loops that show unreasonably large compressive stress near the tangent intersection point. To avoid this undesirable circumstance, the negative slope of a line joining the minimum strain point to the yielding point in compression is used as the target stiffness, which is again not allowed to exceed 3% of the Young's modulus.

The reloading stiffness from the post-buckling compression state is significantly smaller than the Young's modulus E_s due to the gradual loss of axial stiffness in the post-buckling stage. The stiffness of a buckled bar comes mainly from flexure, and the axial stiffness fully participates only after the bar is straightened [44]. To take this in account the reduced reloading stiffness E_b from compression envelope is computed as in the reference [48]:

$$E_b = E_s\left(\frac{\sigma_{\min}}{\sigma_{t\min}}\right)^2 \qquad \mathrm{E_b} \le \mathrm{E_s} \qquad \text{for } \varepsilon_R \le -\varepsilon_y \tag{20}$$

where σ_{min}, σ_{tmin} are respectively the stresses at the minimum strain point in the compression envelope and tension envelope plotted in the compression side.

For a strain reversal from the post-yield region in tension envelope, the unloading stiffness E_u is also reducing. The rate of decrease is especially rapid after yielding, but stabilizes at larger strains. Following the equation from the work presented in [39], the interrelationship between the unloading stiffness E_u normalized with respect to the Young's modulus E_s and the maximum plastic tensile strain ε_m is expressed as:

$$\frac{E_u}{E_s} = 0.82 + \frac{1}{5.55 + 1000\varepsilon_m} \tag{21}$$

Both unloading stiffness E_u and reloading stiffness E_b are updated once the maximum tensile strain respectively minimum compressive strain are exceeded and kept in memory. They are used for all loading/unloading loops to facilitate the path-depending computation (Figure 17).

4.1.4 Matching with the envelope

The Giuffre-Menegotto-Pinto model is combined with tension and compression envelope to formulate a general path-dependent cyclic stress-strain relationship for reinforcing bars. The cyclic loops describe the response until the previously maximum-minimum strain point, after which the response for continuous loading in same direction follows the corresponding envelope. It is observed that the stress at the target point (previously maximum/minimum strain point) in the cyclic loops is less than in the corresponding envelope.

The method used in the algorithm developed in this work to correct this error consists in 2 steps described in the following and shequematically represented in Figure 16. First, when a new loop starts the error which will occur at the target point, is calculated, shifting the stress at that point with the error above the envelope and calculate again the intersection points as shown in the Figure 16. This ensure that, when the loop complete the stress at the target point is very close to the envelope stress, and if, the loading is continued further in the same direction, there will be no sudden jump which may cause convergence problems during FEM iterations. Second, because of high slenderness ratio the reloading stiffness E_b can have a low value that may cause, at the target point, a high difference between the stresses from the cyclic loop and envelope, to avoid the stress shift if the loading continues further in same direction, a linear deduction of this stress shift is deducted from the envelope stress until the difference is nullified at $5\varepsilon_y$ ahead of the target point.

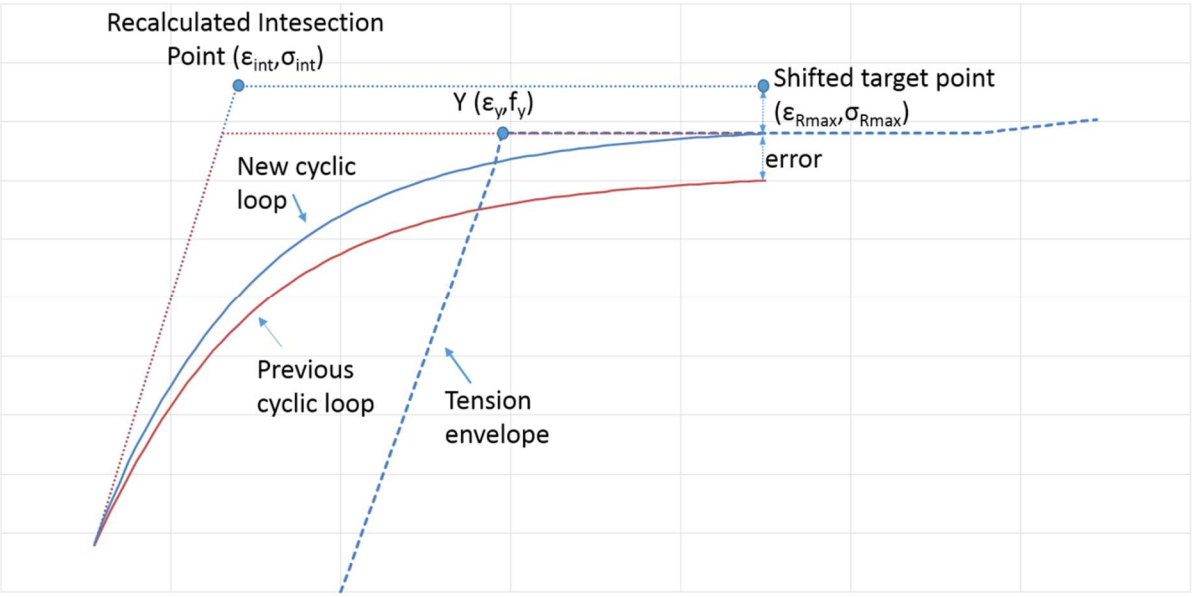

Figure 16 Target point shift

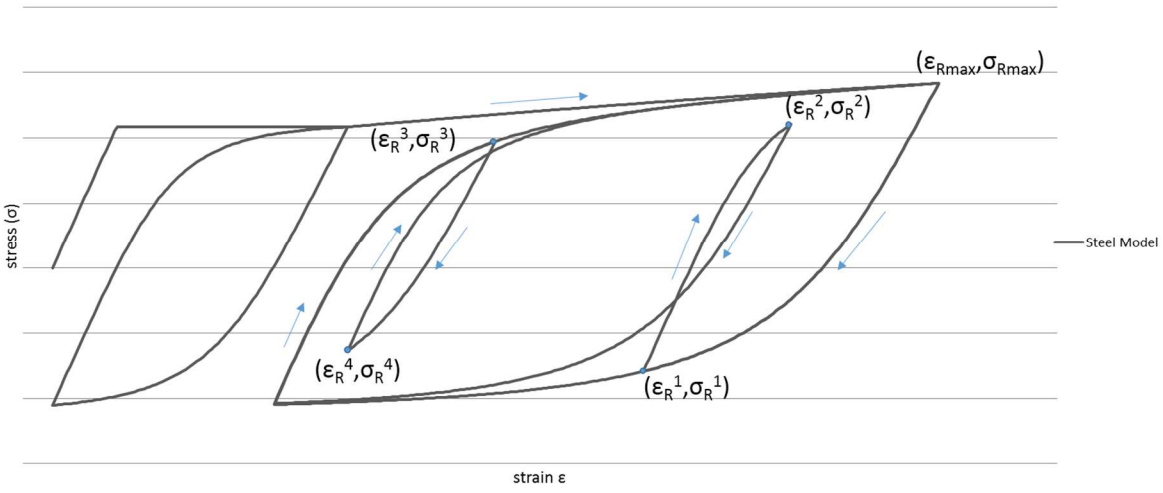

Figure 17 Path depending for random strains reversal

4.3 Algorithm developed to implement the new constitutive model for steel

In the following, the algorithm developed to implement the constitutive model for steel, is described in detail. The equations refer to the description of the model presented in the previous sections of this chapter. At the end, some notes about the meaning and flow of the algorithm are given. The code in Visual Basic is presented as Annex of this document.

Input:

- material constants: f_y ,f_u, f_{sh1}, ε_y, ε_{sh}, ε_u, ε_{sh1}, E_0, R_0, a_1, a_2;
  f_{yn} ,f_{un}, ε_{yn}, ε_{shn}, ε_{un};
- rebar slenderness: L, D.
- variables:
  - buckling : ratio(fi/fit), ε_i, f_i, bk;
  - bauschinger: R, b, ε_{int} ,σ_{int};
  - maximum return points: ε_{Rmax}, σ_{Rmax}, $\sigma_{Rmax\_envelope}$, E_{1poz}, E_{0poz}, ε_{Rmin}, σ_{Rmin}, $\sigma_{Rmin\_envelope}$, E_{1neg}, E_{0neg},
  - return points: ε_{Rpoz}, σ_{Rpoz}, ε_{Rneg}, σ_{Rneg};
  - variable to follow path: i,j,k;
  - error: $error_{poz}$;
- old point: ε, σ, E
- increment: Δε

1. **initialize:**
   $\varepsilon_{old}=\varepsilon$;
   $\sigma_{old}=\sigma$;
   $E_{old}=E$.
2. **compute $\varepsilon=\varepsilon_{old}+\Delta\varepsilon$.**
3. **if (bk=0)**
   compute ε_i using Eq. (11);
   compute α using Eq. (13)
   compute *ratio* and f_i using Eq. (12);
   update bk =1.
4. **if (i=0)**
   if(ε ≥0) (enter on tension envelope)
   if($\varepsilon\leq\varepsilon_y$)
   compute σ using Eq. (1);
   update $E=E_0$.
   elseif (Δε >0)
   if ($\varepsilon\leq\varepsilon_{sh}$)
   compute σ using Eq. (2);
   update E=0,1.
   elseif($\varepsilon\leq\varepsilon_u$)
   compute P using Eq. (5);
   compute σ using Eq. (3);
   compute E using derivative of Eq. (3) and limit ≥0.1 ;
   elseif($\varepsilon>\varepsilon_u$)
   update i=3;

else update i=1;

else (enter on compression envelope)

if($\varepsilon \geq \varepsilon_{yn}$)

compute σ using Eq. (3);

update $E=E_0$;

elseif ($\Delta\varepsilon<0$)

if($\varepsilon \geq \varepsilon_i$)

if ($(-\varepsilon) \leq \varepsilon_{sh}$)

compute σ_t using Eq. (2);

compute E using derivative of Eq. (9).

elseif ($(-\varepsilon) \leq \varepsilon_u$)

compute P using Eq. (5);

compute σ_t using Eq. (3).

compute E using derivative of Eq. (9).

else: update i=3.

if (i<3)

compute σ using Eq. (9).

elseif($\varepsilon \geq \varepsilon_{un}$)

compute σ using Eq. (10) and limit it;

compute E using derivative of Eq. (10).

else: update i=3.

else: update i=1

5. if (i=1)

if ($\Delta\varepsilon<0$)

update $\varepsilon_{Rmax} = \varepsilon_{Rpoz} = \varepsilon_{old}$;

update $\sigma_{Rmax} = \sigma_{Rpoz} = \sigma_{Rmax\_envelope} = \sigma_{old}$;

update $E_{1poz}=E_{old}$;

compute E_{0poz} using Eq. (21)

update $\varepsilon_{Rmin} = \varepsilon_{Rneg} = \varepsilon_{yn}$;

update $\sigma_{Rmin} = \sigma_{Rneg} = \sigma_{Rmin\_envelope} = f_{yn}$;

compute E_{1neg} using derivative of Eq. (9) and limit ≥ 0.1;

update $E_{0neg}=E_0$;

update i=2.

if ($\Delta\varepsilon>0$)

update $\varepsilon_{Rmin} = \varepsilon_{Rneg} = \varepsilon_{old}$;

update $\sigma_{Rmin} = \sigma_{Rneg} = \sigma_{Rmin\_envelope} = \sigma_{old}$;

update $E_{1neg} = E_{old}$ and limit ≥ 0.1;

if($(-\varepsilon_{old}) \leq \varepsilon_{sh}$)

compute σ_t using Eq. (2).

else

compute σ_t using Eq. (3).

compute E_{0neg} using Eq. (20)

update $\varepsilon_{Rmax} = \varepsilon_{Rpoz} = \varepsilon_y$;

update $\sigma_{Rmax} = \sigma_{Rpoz} = \sigma_{Rmax\_envelope} = f_y$;

update $E_{1poz}=0.1$;

update $E_{0poz}=E_0$;

update i=2.

6. if (i=2)

if($\Delta\varepsilon<0$) (unload from tension curve)

(conditions when changing increment)

if (k=1)

update $\varepsilon_{Rpoz} = \varepsilon_{old}$;

update $\sigma_{Rpoz} = \sigma_{old}$;

elseif (k=2)

if ($error_{poz}>0$)

update $\varepsilon_{Rmax} = \varepsilon_{Rpoz} = \varepsilon_{old}$;

update $\sigma_{Rpoz} = \sigma_{old}$;

update $\sigma_{Rmax\_envelope} = f_y$;

compute $\sigma_{Rmax} = \sigma_{Rmax\_envelope} + (\sigma_{Rmax\_envelope} - \sigma_{old})$;

update $E_{1poz}=E_{old}$;

compute E_{0poz} using Eq. (21).

else

update $\varepsilon_{Rmax} = \varepsilon_{Rpoz} = \varepsilon_{old}$;

update $\sigma_{Rmax} = \sigma_{Rpoz} = \sigma_{Rmax\_envelope} = \sigma_{old}$;

update $E_{1poz}=E_{old}$;

compute E_{0poz} using Eq. (21).

elseif (k=3)

if ($error_{poz}>0$)

update $\varepsilon_{Rmax} = \varepsilon_{Rpoz} = \varepsilon_{old}$;

compute P using Eq. (5);

compute $\sigma_{Rmax\_envelope}$ using Eq. (3);

compute $\sigma_{Rmax} = \sigma_{Rmax\_envelope} + (\sigma_{Rmax\_envelope} - \sigma_{old})$;

update $E_{1poz}=E_{old}$;

compute E_{0poz} using Eq. (21).

else

update $\varepsilon_{Rmax} = \varepsilon_{Rpoz} = \varepsilon_{old}$;

update $\sigma_{Rmax} = \sigma_{Rpoz} = \sigma_{Rmax\_envelope} = \sigma_{old}$;

update $E_{1poz}=E_{old}$;

compute E_{0poz} using Eq. (21).

update k=0

if (j=0)

(calculate intersection point Figure 15)

compute ε_{int} and σ_{int};

compute ξ using Eq. (19);

compute R using Eq. (18);

compute b using Eq. (15);

(calculate error at the target point)

compute ε^* using Eq. (16);

compute σ^* using Eq. (14);

compute $\sigma_{return}^{\text{with error}}$ using Eq. (17);

compute $\sigma_{Rmin} = \sigma_{Rmin} + \sigma_{Rmin\_envelope} - \sigma_{return}^{\text{with error}}$;

(calculate again the intersection point)
compute ε_{int} and σ_{int};
compute ξ using Eq. (19);
compute R using Eq. (18);
compute b using Eq. (15);
update j=1.

if ($\varepsilon \geq \varepsilon_{Rmin}$)
compute ε* using Eq. (16);
compute σ* using Eq. (14);
compute σ using Eq. (17);
compute $E = \frac{\sigma - \sigma_{old}}{\varepsilon - \varepsilon_{old}}$;

else (enter on compression envelope)
if($\varepsilon \geq \varepsilon_i$)
update j=2
if ($(-\varepsilon) \leq \varepsilon_{sh}$)
compute σ_t using Eq. (2);
compute E using derivative of Eq. (9).
elseif ($(-\varepsilon) \leq \varepsilon_u$)
compute P using Eq. (5);
compute σ_t using Eq. (3).
compute E using derivative of Eq. (9).
else: update i=3.
if (i<3)
compute σ using Eq. (9).
elseif($\varepsilon \geq \varepsilon_{un}$)
update j=3
compute σ using Eq. (10) and limit it;
compute E using derivative of Eq. (10).
else: update i=3.

if(Δε<0) (unload from compression curve)
(conditions when changing increment)
if (j=1)
update $\varepsilon_{Rneg} = \varepsilon_{old}$;
update $\sigma_{Rneg} = \sigma_{old}$;
elseif (j=2)
update $\varepsilon_{Rmin} = \varepsilon_{Rneg} = \varepsilon_{old}$;
update $\sigma_{Rneg} = \sigma_{Rmin} = \sigma_{Rmin\_envelope} = \sigma_{old}$;
update $E_{1neg} = E_{old}$ and limit ≥0.1;
if ($(-\varepsilon) \leq \varepsilon_{sh}$)
compute σ_t using Eq. (2);
elseif ($(-\varepsilon) \leq \varepsilon_u$)
compute P using Eq. (5);
compute σ_t using Eq. (3).
compute E_{0neg} using Eq. (20)
elseif (j=3)
update $\varepsilon_{Rmin} = \varepsilon_{Rneg} = \varepsilon_{old}$;

update $\sigma_{Rneg} = \sigma_{Rmin} = \sigma_{Rmin\_envelope} = \sigma_{old}$;
update $E_{1neg}=E_{old}$ and limit ≥0.1;
if $((-\varepsilon)\leq\varepsilon_{sh})$
compute σ_t using Eq. (2);
elseif $((-\varepsilon)\leq\varepsilon_u)$
compute P using Eq. (5);
compute σ_t using Eq. (3).
compute E_{0neg} using Eq. (20)
update j=0.
if (k=0)
(calculate intersection point Figure 15)
compute ε_{int} and σ_{int};
compute ξ using Eq. (19);
compute R using Eq. (18);
compute b using Eq. (15);

(calculate error at the target point)
compute ε* using Eq. (16);
compute σ* using Eq. (14);
compute $\sigma_{return}^{with\ error}$ using Eq. (17);
compute $\sigma_{Rmax}= \sigma_{Rmax}+\sigma_{Rmax\_envelope}- \sigma_{return}^{with\ error}$;

(calculate again the intersection point)
compute ε_{int} and σ_{int};
compute ξ using Eq. (19);
compute R using Eq. (18);
compute b using Eq. (15);
update j=1.

if $(\varepsilon\leq\varepsilon_{Rmax})$
compute ε* using Eq. (16);
compute σ* using Eq. (14);
compute σ using Eq. (17);
compute $\mathrm{E}=\frac{\sigma-\sigma_{old}}{\varepsilon-\varepsilon_{old}}$.
if $(\varepsilon=\varepsilon_{Rmax})$
if $(\varepsilon\leq\varepsilon_{sh})$
compute $error_{poz}$=fy-σ.
else $(\varepsilon\leq\varepsilon_u)$
compute P using Eq. (5);
compute $\sigma_{envelope}$ using Eq. (3);
compute $error_{poz}=\sigma_{envelope}-\sigma$.

else (enter on compression envelope)
if $(\varepsilon\leq\varepsilon_{sh})$

update k=2;
compute $error_{poz}$= $error_{poz}$- $error_{poz}$* $\Delta\varepsilon/(5*\varepsilon_y)$.
if ($error_{poz}$>0)
$\sigma = f_y$- $error_{poz}$;
E=0.1.
else
$\sigma = f_y$;
E=0.1.
elseif ($\varepsilon \leq \varepsilon_u$)
update k=3;
compute $error_{poz}$= $error_{poz}$- $error_{poz}$* $\Delta\varepsilon/(5*\varepsilon_y)$.
if ($error_{poz}$>0)
compute P using Eq. (5);
compute σ using Eq. (3) - $error_{poz}$;
compute E using derivative of Eq. (3) and limit ≥0.1.
else
compute P using Eq. (5);
compute σ using Eq. (3);
compute E using derivative of Eq. (3) and limit ≥0.1.
else
update i=3.

Output:

ε , σ and E.

Notes about the algorithm:

- *bk* variable is used to compute the intermediate point (ε_i, only once at the first run of the algorithm.
- Limiting tangential stiffness (E for positive envelope) to be no less than 0.1 because lower values can cause convergence problems in FEM iterations.
- Path dependent variable "i":
  - It remains 0 until the first strain reversal from a post elastic incursion and then update it to 1.
  - 1 is used to store the return points and stiffness depending if unload occurs from tension or compression side and update it to 2;
  - while "i" is equal to 2, cyclic loops model is used until $\varepsilon=\varepsilon_{max}$, then the model follows the envelope.
  - when "i" reaches 3 the ultimate strain was reached.

- Path dependent variable “j” is used for negative value of increment (Δε<0) when unloading from the post-yield region in tension side (Figure 18). Using this parameter the return points are updated immediately after the strain reversal takes place:
  - j=1 - means the strain reversal occurred before the previous minimum return strain was reached (ε_{Rmin});
  - j=2 - means the strain reversal occurred after the minimum return strain (ε_{Rmin}) and before the intermediate point was reached (ε_I);
  - j=3 - means the strain reversal occurred before ultimate strain point was reached (ε_u).

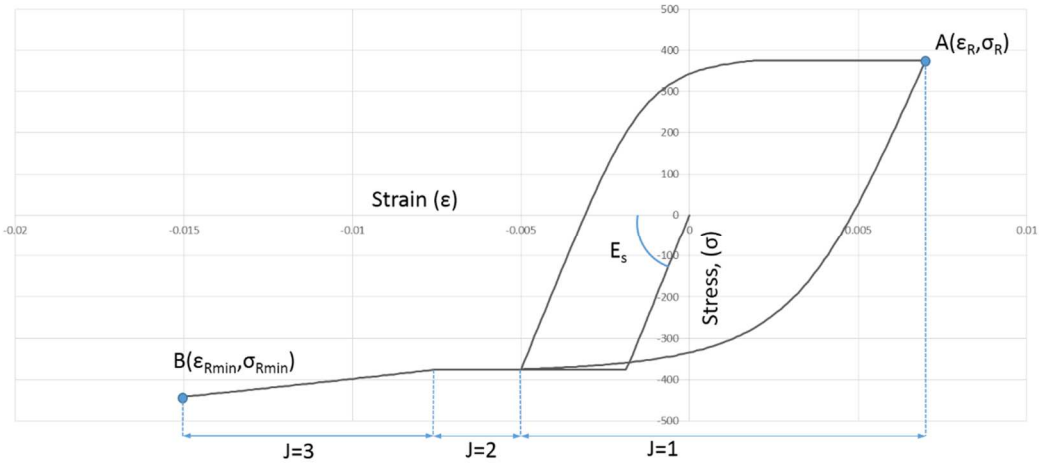

Figure 18 Variation of the "j" parameter

- Path dependent variable “k” it’s used for positive value of increment (Δε>0) when unloading from the post-yield region in compression side (Figure 19). By using this parameter, the return points are updated immediately after the strain reversal takes place:
  - k=1 - means the strain reversal occurred before the previous maximum return strain was reached (ε_{Rmax});
  - k=2 - means the strain reversal occurred before the strain hardening strain was reached ($\varepsilon_{sh)}$ and after the previous maximum return strain (ε_{Rmax});
  - k=3 - means the strain reversal occurred before ultimate strain point was reached (ε_u).

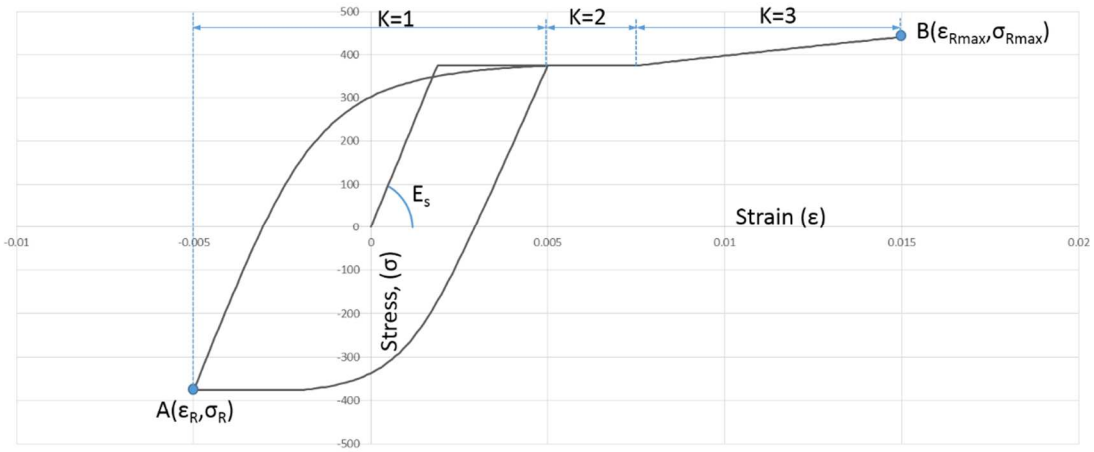

Figure 19 Variation of the "k" parameter

4.4 Verification of the implementation of the algorithm

The performance of the algorithm was evaluated using the cyclic test results of Monti and Nuti [44] which include buckling and also strain reversal after buckling occurred.

The three "S" tests consist in 3 symmetrical single loops of increasing amplitude but with different slenderness ratio (L/D = 5, 8, 11).

The three "C" tests consists in non-symmetrical loading tests of specimens with same slenderness (L/D = 11) but slightly different materials properties.

Material properties and the strain history followed in each test are listed in Table 1.

The branch parameters: R_0= 20, a_1 = 18.5 and a_2 = 0.15 were assumed or this tests.

Test	L/D	f_y [MPa]	E_s (Gpa)	ε_{sh} [%]	ε_{sh1} [%]	f_{sh1} [MPa]	Strain history
C1	11	470	200	0.7	4	660	+0.5 -0.5 +2.5 –1 +2 +0.4 +4 +1 +3 +1.5 +4
C2	11	470	200	0.7	4	660	+1 0 +1.5 -0.5 +2 -0.5 +4 +1.5 +3 +0.5 +4
C5	11	430	160	1.0	4	580	+1 –1 +2 –1 +3 –1 +4 -3
S5	5	500	200	0.7	2	630	1 -1 +2 -2 +3 -3
S8	8	500	200	0.7	2	630	1 -1 +2 -2 +3 -3
S11	11	500	200	0.7	2	630	1 -1 +2 -2 +3 -3

Table 1 Material properties and strain history followed in each test

In the following figures (Figure 19 to Figure 30) each experimental stress –strain curve is compared with the algorithm results. To emphasize the importance of buckling, experimental curves are also compared with a cyclic model that is not affected by the buckling (low L/D ratio). Tensile and compression envelopes are also included for comparison.

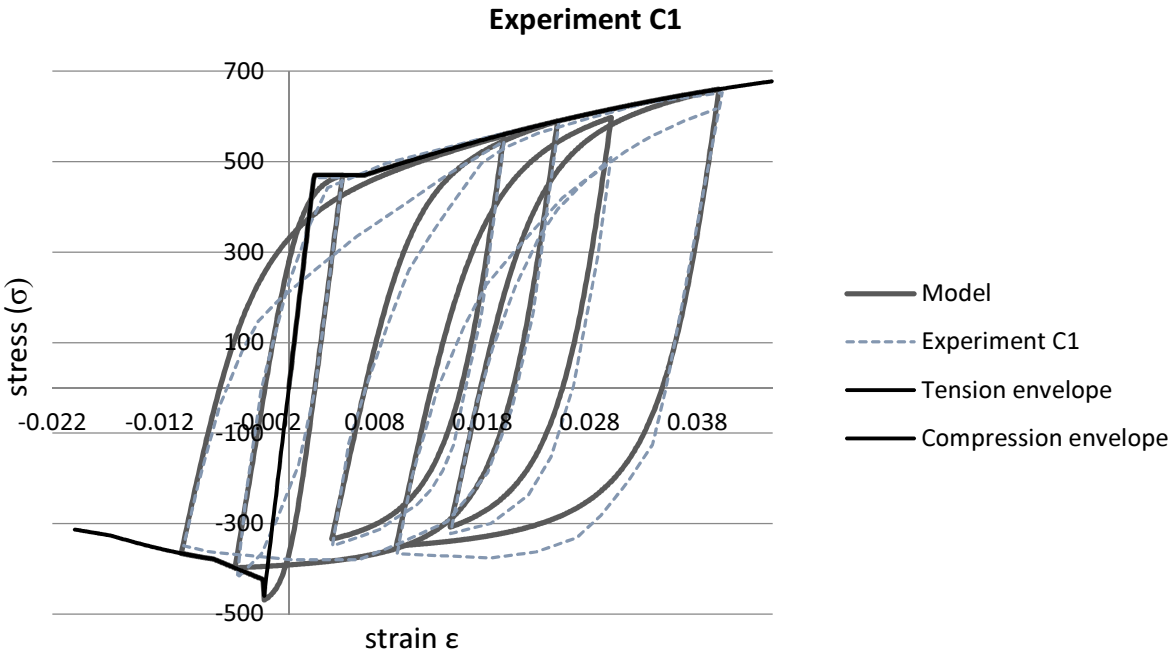

Figure 20 Experiment C1 including buckling

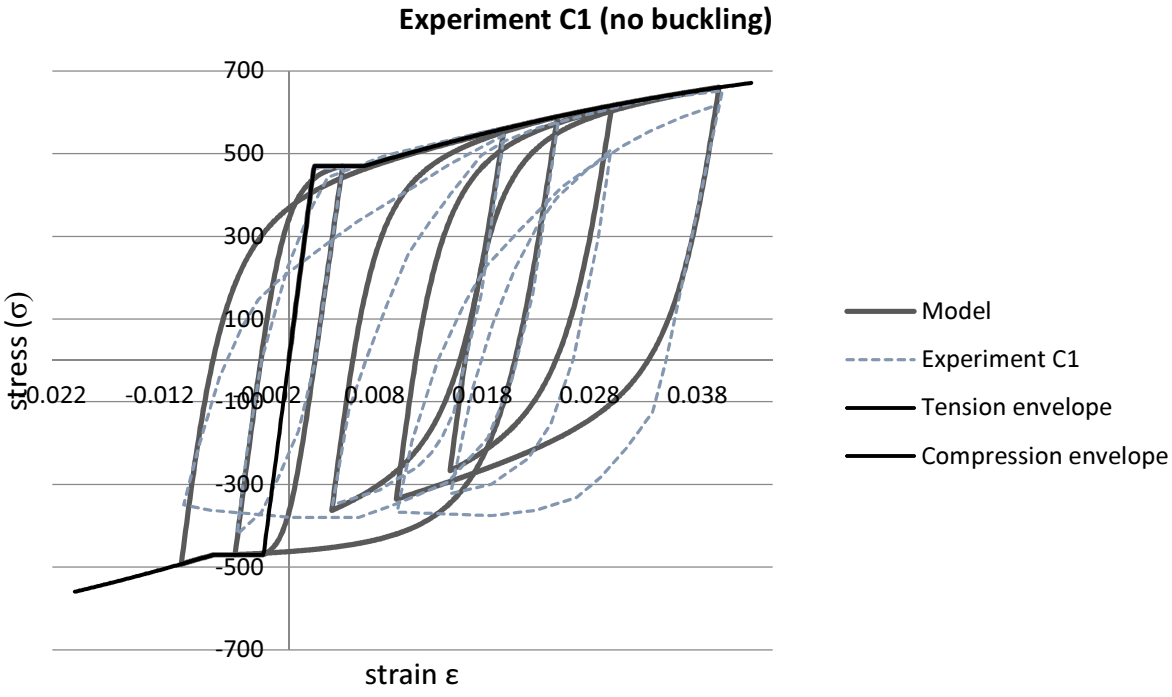

Figure 21 Experiment C1 without buckling

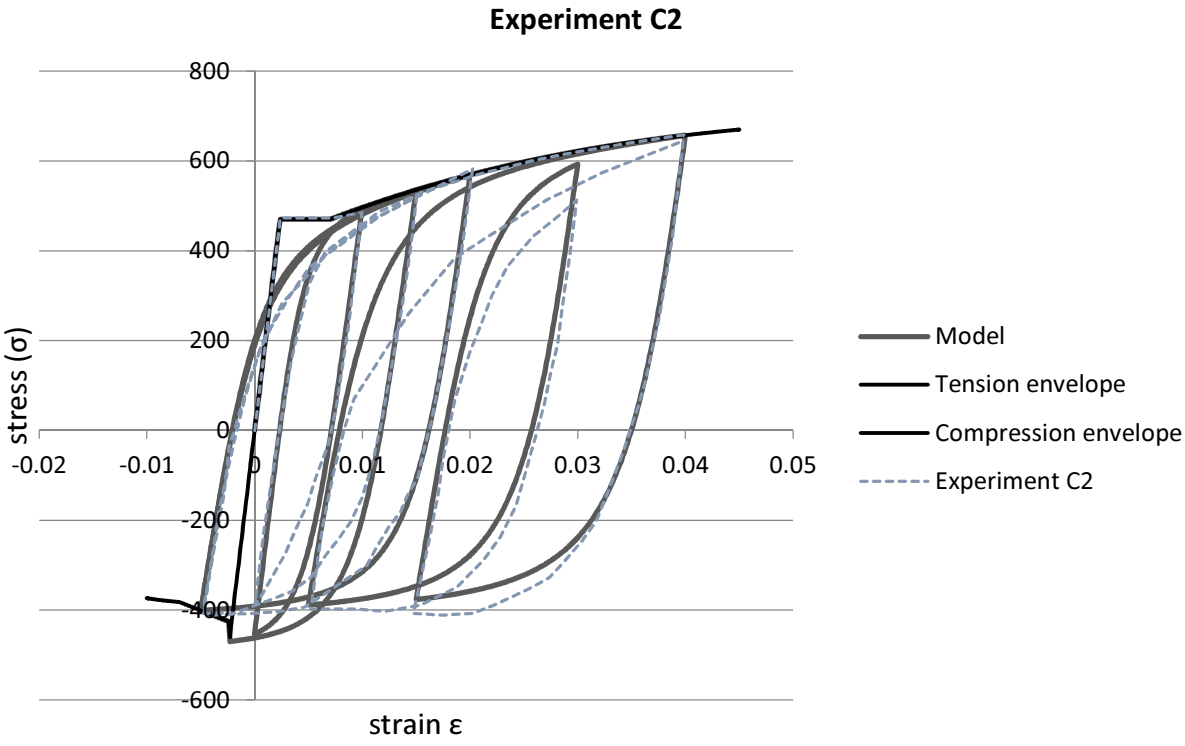

Figure 22 Experiment C2 including buckling

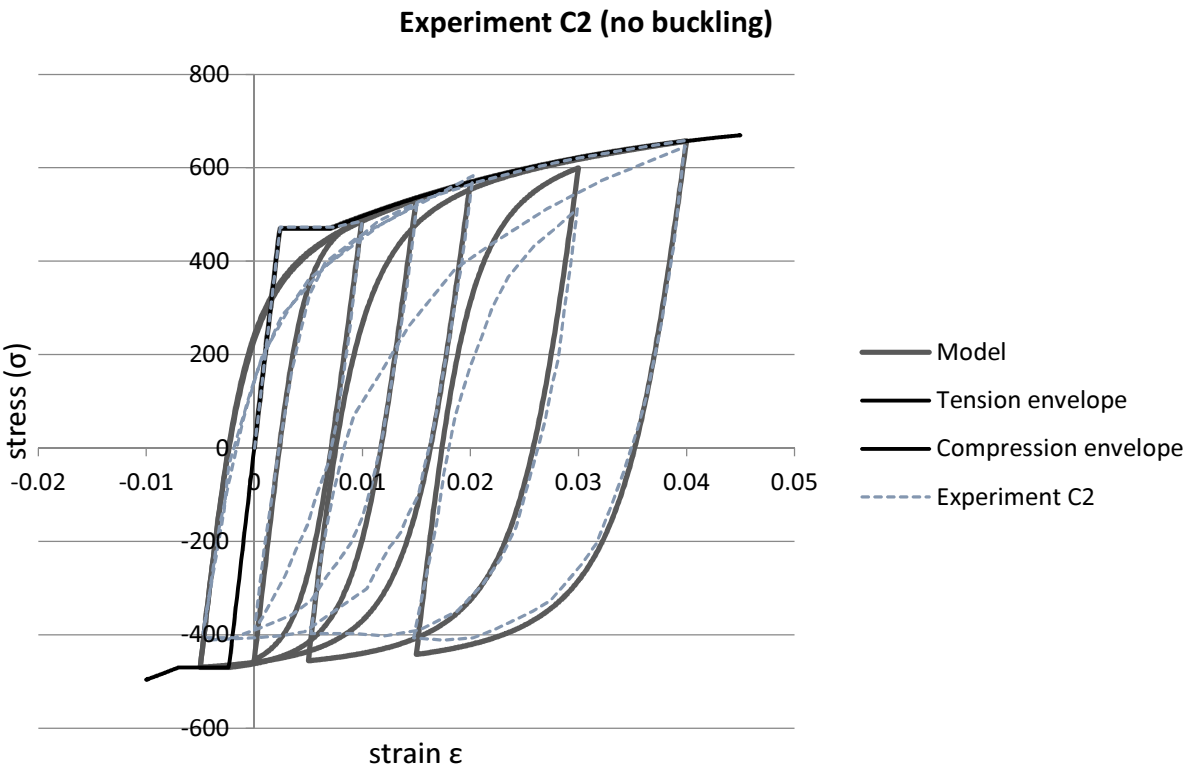

Figure 23 Experiment C2 without buckling

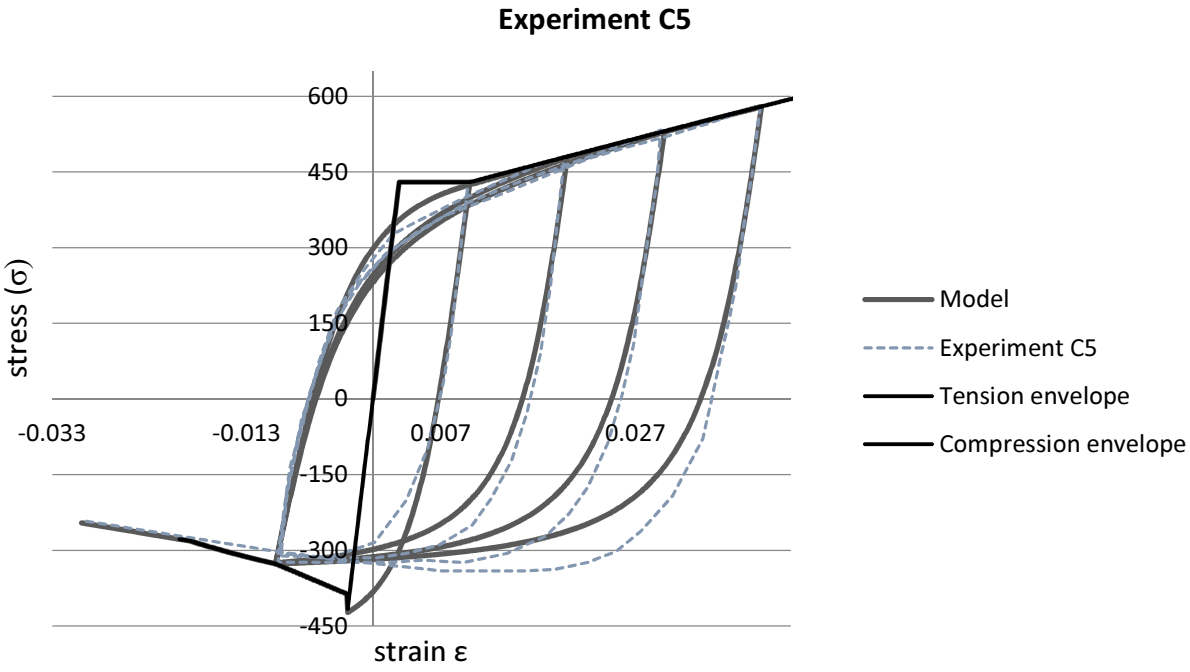

Figure 24 Experiment C5 including buckling

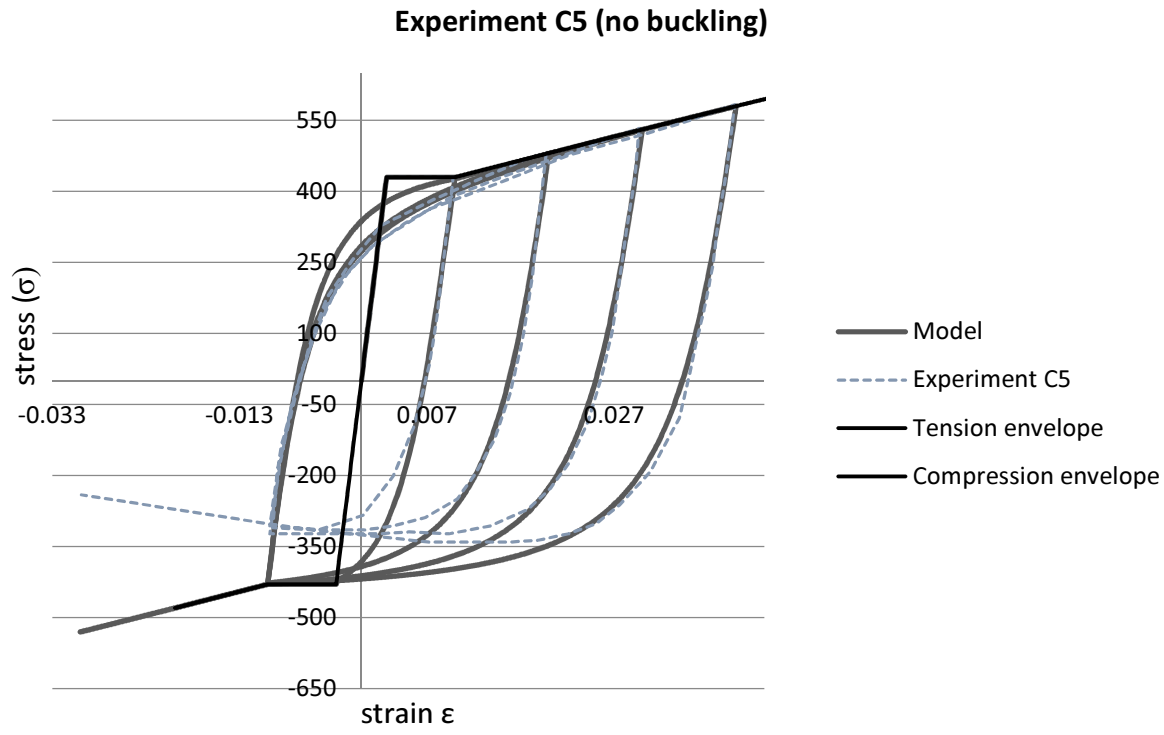

Figure 25 Experiment C5 without buckling

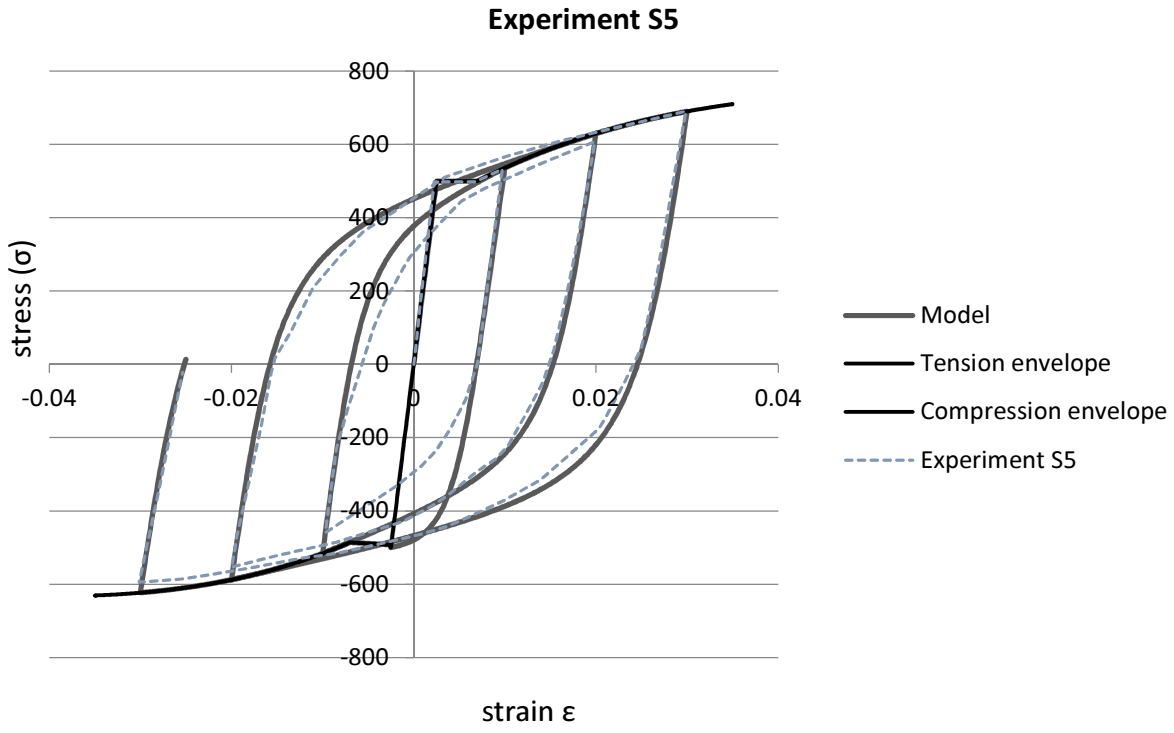

Figure 26 Experiment S5 including buckling

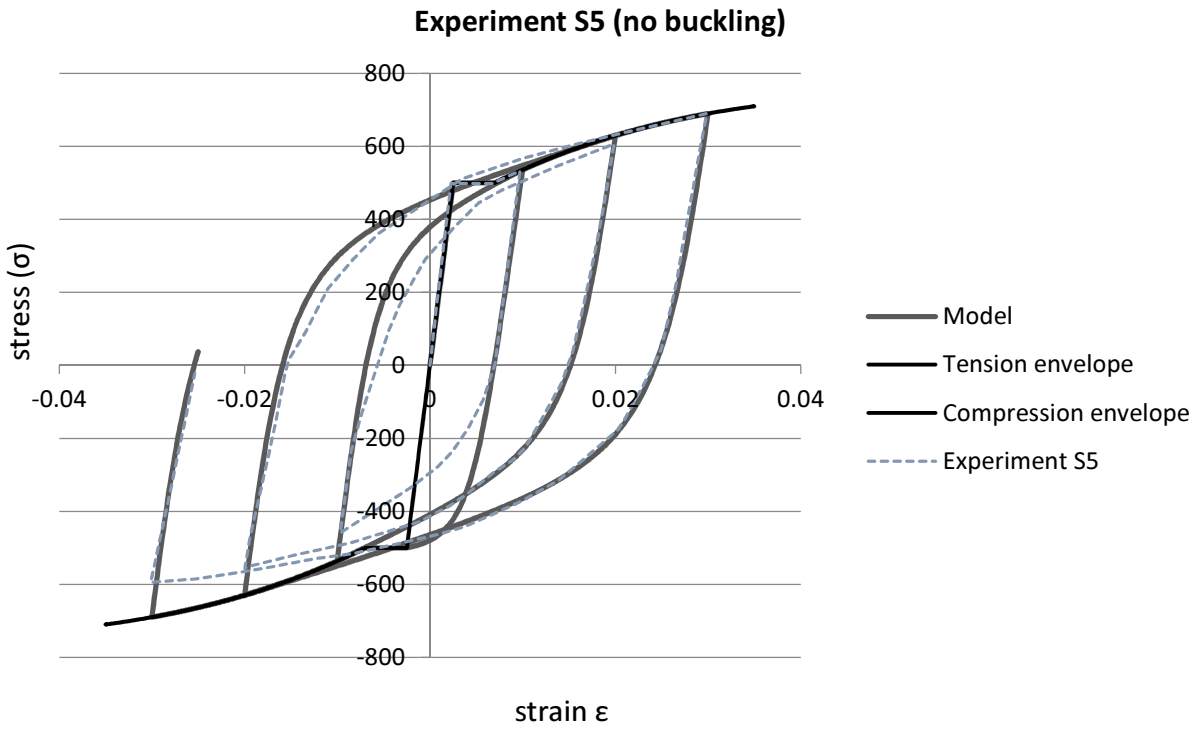

Figure 27 Experiment S5 without buckling

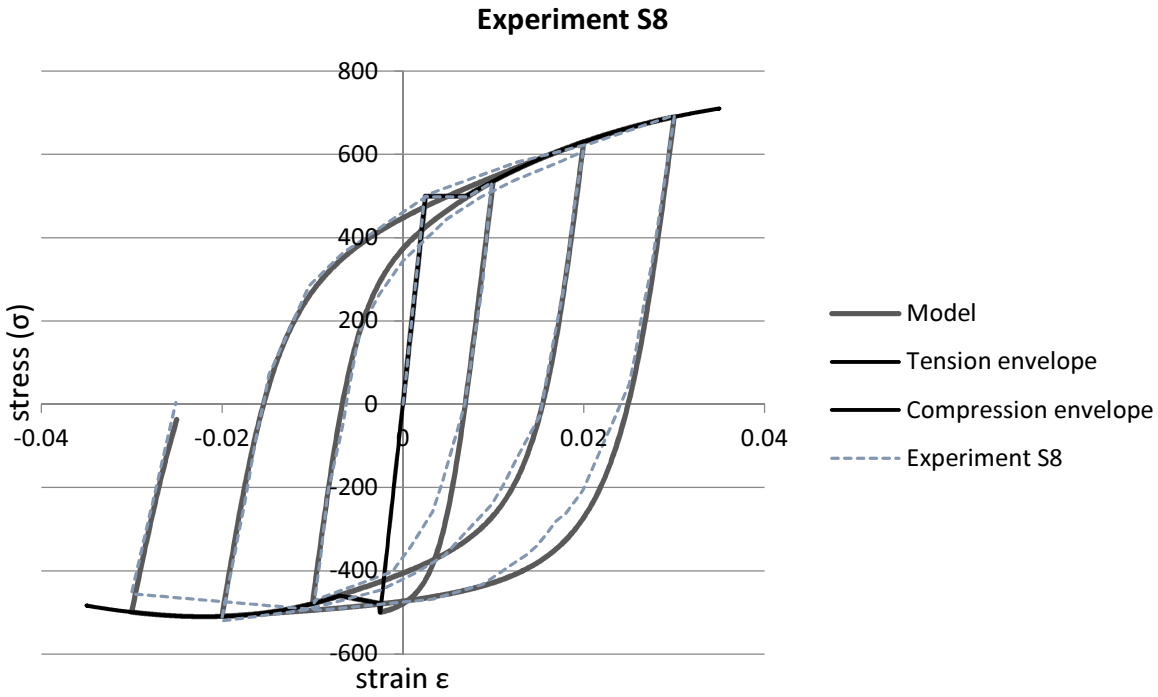

Figure 28 Experiment S8 including buckling

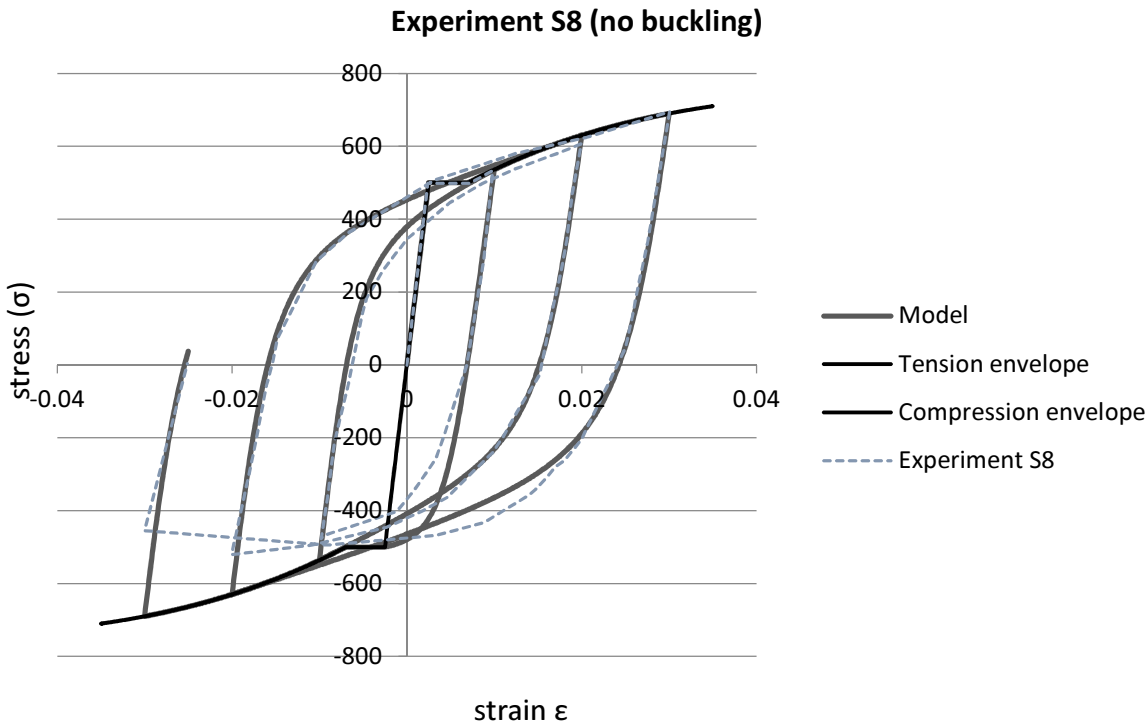

Figure 29 Experiment S8 without buckling

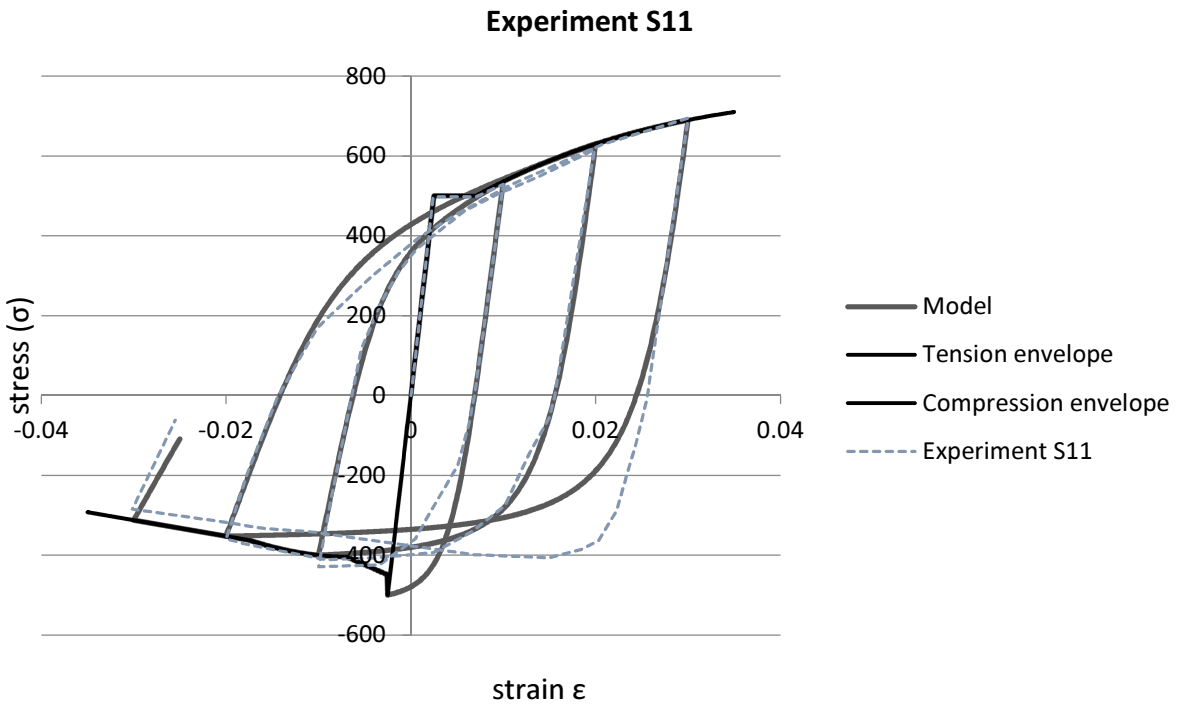

Figure 30 Experiment S11 including buckling

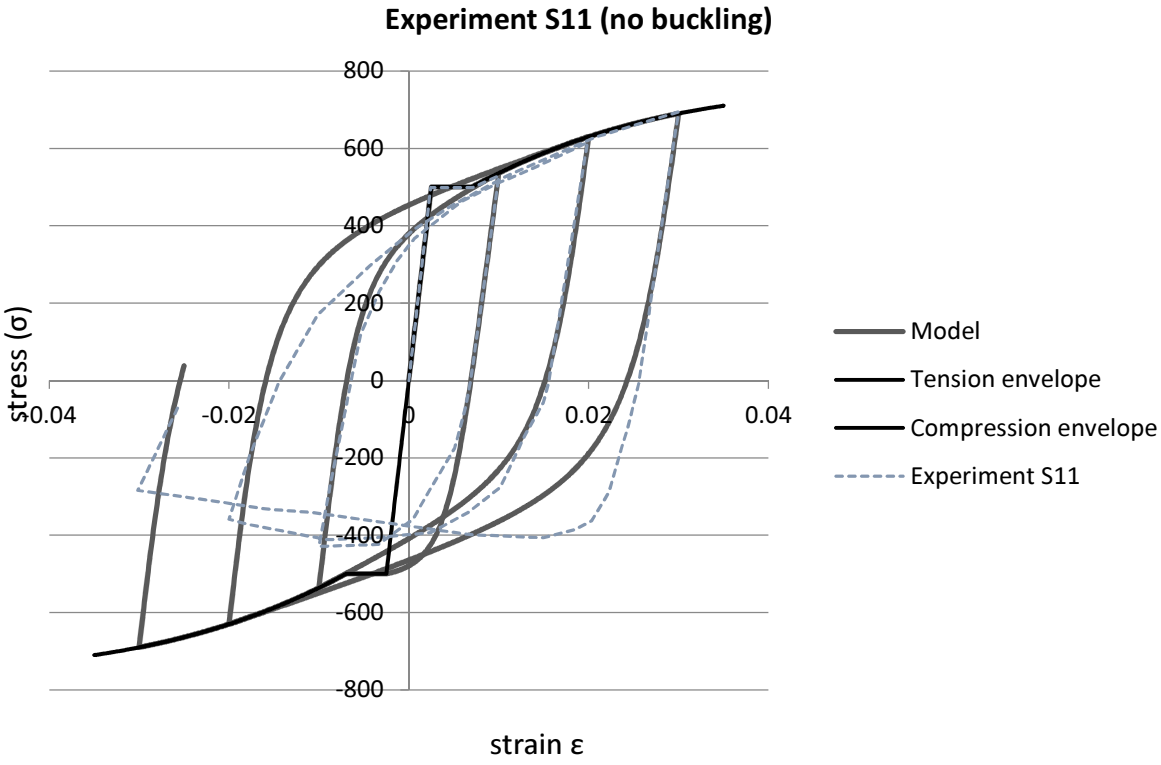

Figure 31 Experiment S11 without buckling

From the presented results the following aspects were observed:

- in case of low slenderness ratio (L/D=5) the experimental and numerical curves are very similar, because the bar was barely influenced by buckling (observed in Figure 26 and Figure 27);
- for the case of the bar with slenderness ratio 8 and 11, the model curves deviate from the experimental results, especially in compression side, where large overestimations of stresses are observed, (Figure 28 to Figure 31);
- the curves predicted by the model fit the experimental ones, with reliable path depending results. The cyclic loops path and compressive softening after buckling can be satisfactorily captured by the model. This was observed in general in all the examples.

4.5 Implementation

The algorithm has been implemented into ConShear (Figure 32). The algorithm (originally written in Visual Basic language was adapted to Fortran77 in which ConShear is written.

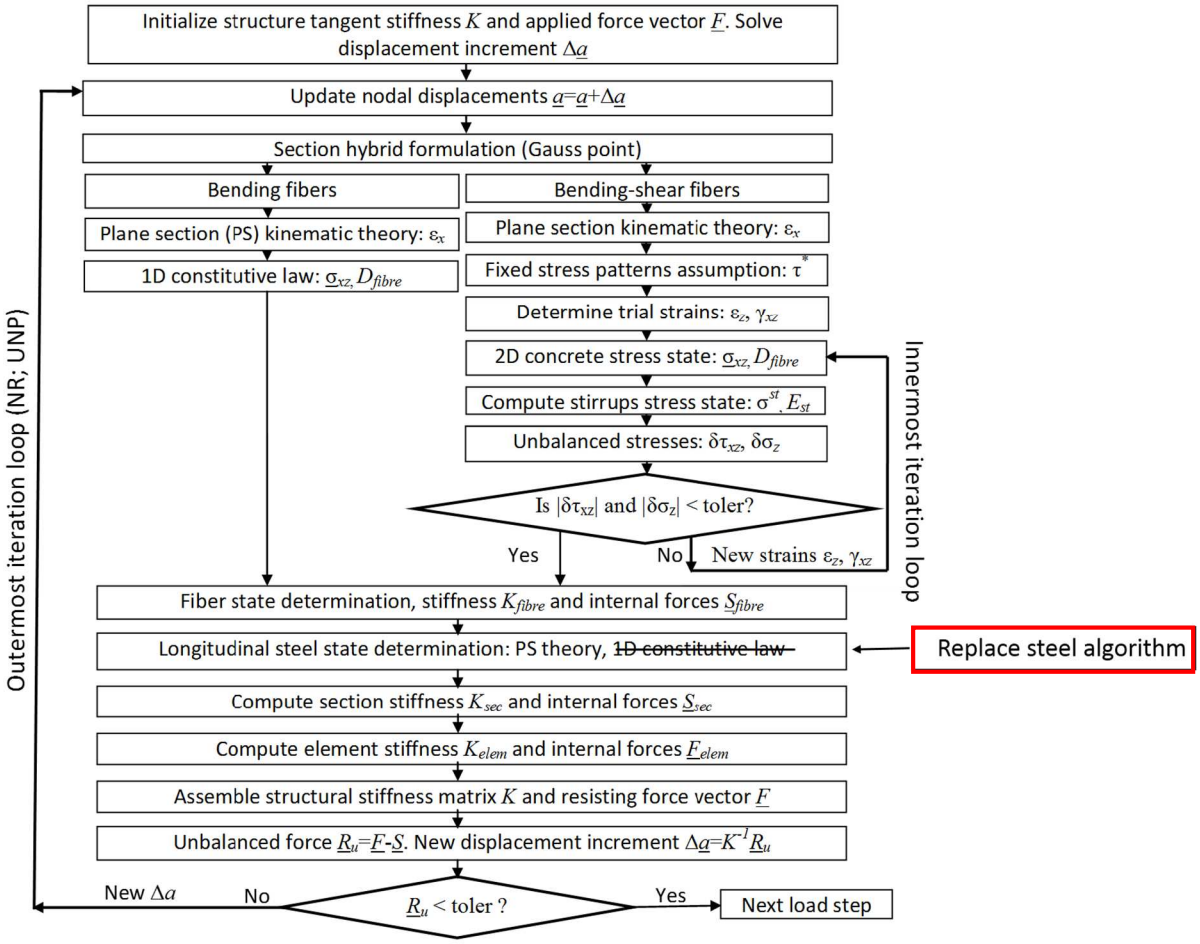

Figure 32 Change in ConShear flow chart

5 Verification of the numerical model

The experimental test, column SC3 analyzed by Morh (REF), was simulated on monotonic loading on the weak direction with CONSHEAR including new steel model (Figure 32). The detailed informations on the experimental campaign that include this specimen are available in web site [63].

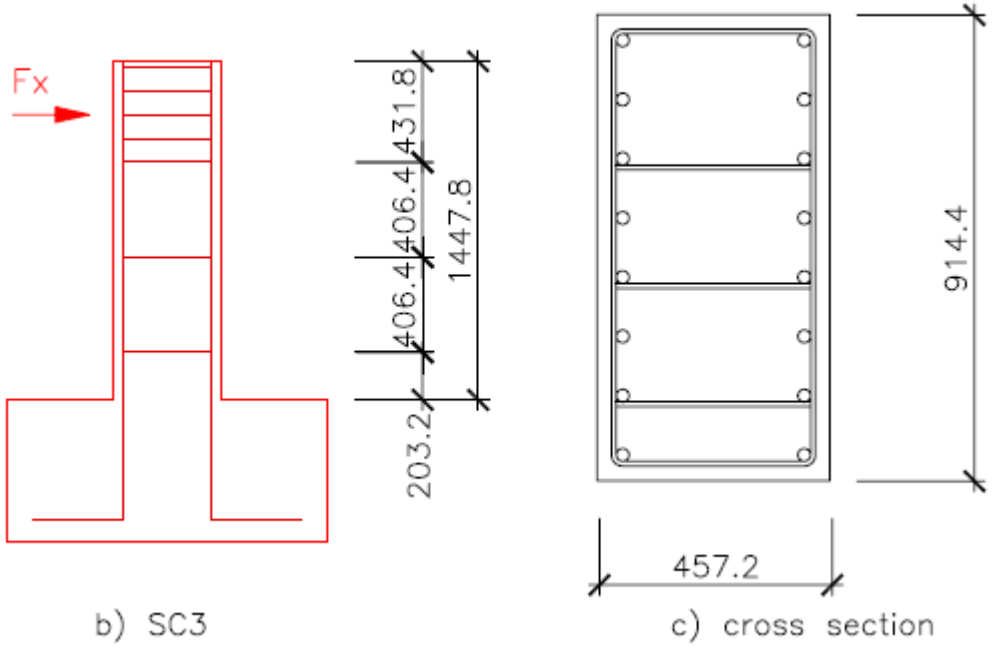

Figure 33 Column figure and reinforcement [28]

Load-displacement curve computed by the model is compared with the envelope of experimental results. This example shows that the model with the new steel subroutine is working and presents good results. Next set would be running this benchmark under cyclic loading.

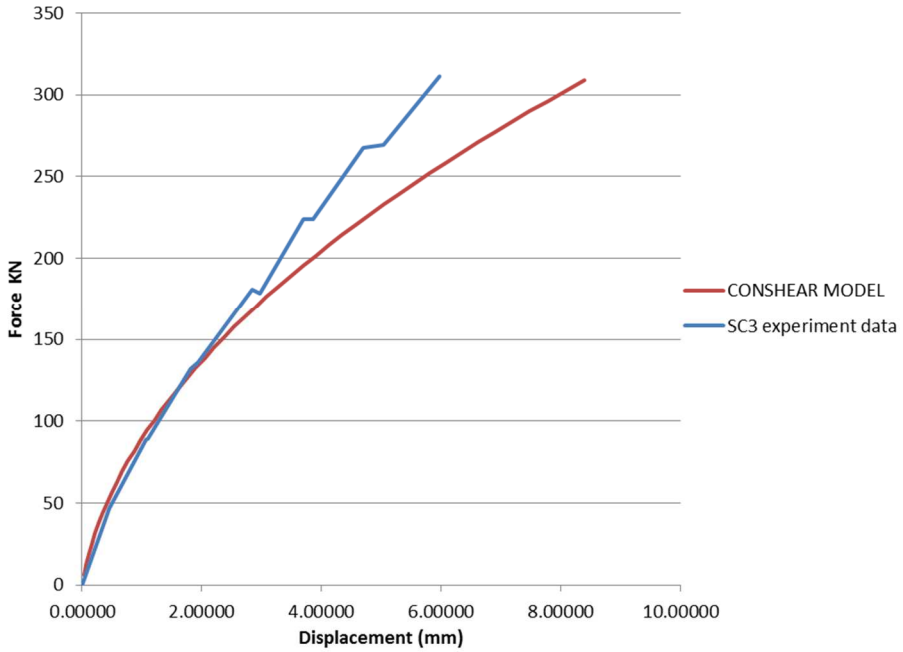

Figure 34 Load-displacement for column SC3

The steel model was tested to cyclic loading with CONSHEAR on a small example, a one element cantilever for one unloading cycle (Figure 34). The results for strain-stress state of reinforcement are presented in Figure 36.

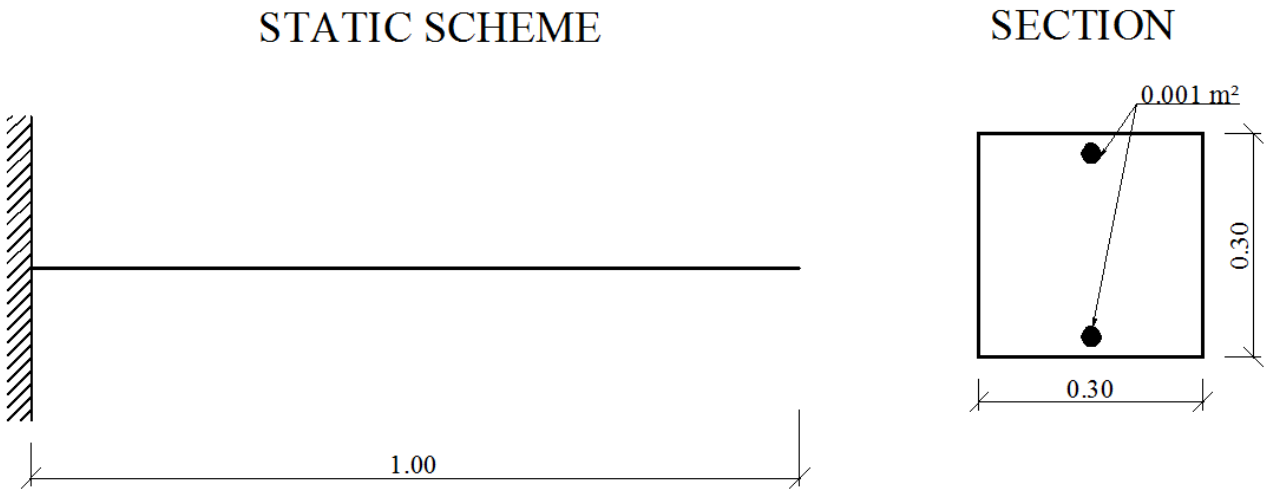

Figure 35 Small test of one element cantilever under cyclic lateral loading: a) Static Scheme b) Cross-section

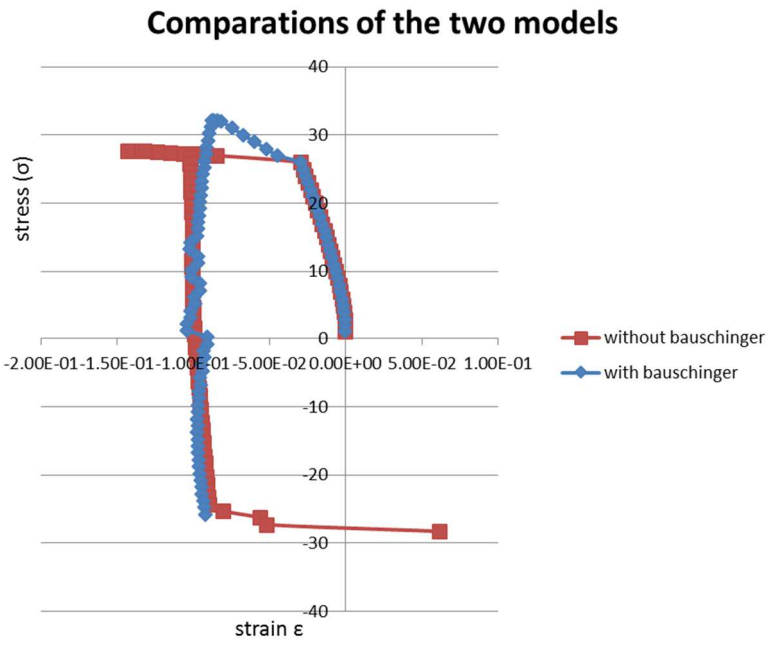

Figure 36 Strains vs stresses response of the longitudinal reinforcement

The results are looking promising but the model isn't robust enough to test on more than one unloading. This make a good theme for future work, on improving the solution procedures

6 Conclusions and future work

This thesis presented a constitutive model for reinforcing steel accounting for the Bauschinger and buckling effects; which are important phenomena that need to be considered in nonlinear cyclic analysis of RC columns. This work was centered on the development of an algorithm for the constitutive law of steel and its validation with experimental results available in literature of rebars under cyclic loading. Afterwards this new algorithm was implemented into an existing FE code based on the fibre beam formulation with enhanced capabilities regarding accounting for shear effects in the nonlinear response of RC structures.

From this work the following conclusions can be drawn:

- For nonlinear cyclic analysis of RC elements it is very important to include the Bauschinger and buckling effects in order to ensure adequate analysis.
- The models considered in this thesis from Maekawa and Dhakal [48] for compression envelope, Giuffre - Pinto [50] and Menegotto - Pinto [51] model for cyclic loops which was improved by Filippou et all [40] present a very good fitting with experimental data.
- A new correction was implemented, which consist in calculating the error at the target point when a new loop starts and computing new intersection points by shifting the stress at that point with the error above the envelope, showing good performance.
- The model is able to reproduce the buckling of rebars in compression.
- The results computed by the model used in this thesis were verified against experimental data of different types tests, including, various types of steels, diameters and loading settings, and the computed results showed consistently very good agreements with the experiments.
- This validation ensured that the algorithm for the constitutive law of steel developed in this thesis is correct and can be implemented into any FE code for nonlinear cyclic analysis.
- From the preliminary set of examples made to verify the implementation into the FE code, the results are very promising, being able to represent Bauschinger effects in cyclic analysis.

This work opened several different lines of research that can be continued in the future:

- Perform a deep validation of the fibre beam model with the new constitutive law for steel by performing a systematic set of analysis of benchmarks available in literature.
- Work on the implementation of enhanced solution methods for the nonlinear model in order to increase the computational robustness when dealing with cyclic loading.

- Study the effects of shear in RC columns and the importance of accounting for shear effects in the numerical analysis.
- Use the model for real scale applications for analysis and assessment of RC columns under seismic loading.
- Adapt the model to probabilistic frameworks and perform reliability analysis concerning the response of RC columns under cyclic loading.
- Use the validated software for performing parametric numerical studies and contributing to sharpen design methodologies and analytical models.

References:

[1] "www.encipedia.org." .

[2] E. O. Bustamante, "Efectos de los esfuerzos cortantes biaxiales en la respuesta sísmica de columnas de hormigón armado," 2012.

[3] P. G. Bergan, G. Horrigmoe, B. Brrakeland, and T. H. Søreide, "Solution techniques for non−linear finite element problems," *Int. J. Numer. Methods Eng.*, vol. 12, no. 11, 1978.

[4] D. P. Mondkar and G. H. Powell, "Evaluation of solution schemes for nonlinear structures," *Computers & Structures*, vol. 9, no. 3. pp. 223–236, 1978.

[5] M. J. Clarke and G. J. Hancock, "A Study of Incremental-Iterative Strategies for Non-Linear Analyses." Int. J. Numer. Methods Eng., 29(7), pp. 1365–1391, 1990.

[6] Y.-B. Yang and M.-S. Shieh, "Solution Method for Nonlinear Problems with Multiple Critical Points," *AIAA J.*, vol. 28, no. 12, pp. 2110–2116, 1990.

[7] M. Rezaiee-Pajand, M. Tatar, and B. Moghaddasie, "Some Geometrical Bases for Incremental-Iterative Methods." Int. J. Eng. Trans. B: Appl., 22(3), pp. 245–256, 2009.

[8] R. Clough and S. Jhonston, "Effect of Stiffness Degradation on Earthquake Ductility Requirements." Transactions of Japan Eartquake Engineering Symposium Tokyo, pp. 195–198.

[9] M. F. Giberson, "The Response of Nonlinear Multi-story Structures Subjected to Earthquake Excitation," 1967.

[10] Takizawa H., "Notes on Some Basic Problems in Inelastic Analysis of Planar RC Structures." Transactionss of AIJ, pp. Part I: Feb 51–62; Part II:March 65–67, 1976.

[11] R. Clough and L. Benuska, "Nonlinear EarthquakeBehavior of Tall Buildings." Journal of Mechanical Engineering ASCE, 93 (EM3), 129-146, 1967.

[12] T. Takeda, M. A. Sozen, and N. N. Nielsen, "Reinforced Concrete Response to Simulated Earthquakes," *J. Struct. Div.*, vol. 96, no. 12, pp. 2557–2573, 1970.

[13] F. Brancaleoni, V. Ciampi, and R. Di Antonio, "Rate-Type Models for Non Linear Hysteretic Structural Behavior." EUROMECH Colloquim, Palermo.

[14] H. Banon, H. M. Irvine, and J. M. Biggs, "Seismic Damage in Reinforced Concrete Frames," *J. Struct. Div.*, vol. 107, no. 9, pp. 1713–1729, 1981.

[15] Filip C. Filippou and Ahmad Issa, "NONLINEAR ANALYSIS OF REINFORCED CONCRETE FRAMES UNDER CYCLIC LOAD REVERSALS," 1988.

[16] D'Ambrisi A. and F. C. Filippou, "Correlation studies on a RC Frame Shaking-table specimen.," *Earthquake Engineering and Structural Dynamics, 26 (10), 1021-1040,*. 1997.

[17] I. G. Buckle and A. T. Jackson, "A filamented beam element forthe nonlinear analysis of reinforced concret shells with edge beams." Department of Civil Engineering, University of Auckland, New Zealand.

[18] Mahasuverachai M. and G. H. Powel, "inelastic Analysis of Piping and Tubular Structures." EERC Report 82/27, Earthquake Engineering Research Center, University of California, Berkeley, 1982.

[19] S. Kaba and S. A. Mahin, "Refined Modeling of Reinforced Concrete Columns for Seismic Analysis." EERC Report 84/03, Earthquake Engineering Research Center, University of California, Berkeley.

[20] E. C. Chan, "Nonlinear geometric material and time dependent analysis of reinforced concrete shells with edge beams." Report UCB-SESM 82/8. University of California, Berkeley.

[21] A. R. Mari, "Nonlinear geometric,material and time dependent analysis of three dimensional." Structural Engineering and Structural Mechanics, Department of Civil Engineering, University of California, Berkeley, CA., 1984.

[22] F. J. Ulm, J. L. Clement, and J. Guggenberger, "Recent Advances in 3D nonlinear FE-analysis of R/C and P/C beam structures." Proc ASCE Structures Congress XII, Atlanta (USA), 1427-1432.

[23] M. Petrangeli and V. Ciampi, "Equilibrium Based Iterative Solutions For The Non-Linear Beam Problem," *Int. J. Numer. Methods Eng.*, vol. 437, no. February 1996, pp. 423–437, 1997.

[24] E. Spacone, F. C. Filippou, and F. F. Taucer, "Fibre Beam-Column Model for Non-linear Analysis of R/C Frames: Part 1. Formulation," *Earthq. Eng. Struct. Dyn.*, vol. 25, no. 7, pp. 711–725, 1996.

[25] A. Saritas and F. C. Filippu, "A beam finite element for shear critical RC beams." ACI Special Publication SP-237, 295-310, 2006.

[26] M. Petrangeli, P. E. Pinto, and V. Ciampi, "Fiber Element for Cyclic Bending and Shear of RC Structures. I: Theory," *Journal of Engineering Mechanics*, vol. 125, no. 9. pp. 994–1001, 1999.

[27] J. M. Bairan and A. R. Mari, "Proyecto de estructuras de hormigón armado con armaduras de alta ductilidad," 2007.

[28] S. Mohr, "Nonlinear static and dynamic model for the analysis of reinforced concrete frames under high shear forces Doctoral Thesis : Nonlinear static and dynamic model," no. March, 2010.

[29] A. R. Marí, "Numerical simulation of the segmental construction of three dimensional concrete frames," *Engineering Structures*, vol. 22, no. 6. pp. 585–596, 2000.

[30] S. Carrascon, A. R. Mari, and I. Carol, “Instantaneous and time-dependent analysis of reinforced and prestressed concrete curve bridges.” Technical Report Publication ES-015, Universitat Politecnica de Catalunya, Department d’Enginyeria de la Construccio, Barcelona, 1987.

[31] I. Carol and J. Murcia, “Nonlinear time-dependent analysis of planar frames using an exact formulation - I theory.” Computers & Structures, 33(1), pp. 79–87, 1989.

[32] A. R. Mari, “Estudio Comparativo entre diversos metodos de analisis no lineal de estructuras reticulares de hormigon armado y pretensado: Estado actual y lineas de futura actuacion. Modelos de Analisis de estructuras de Hormigon.” GEHO, Comision II, Madrid, 1991.

[33] CEB, “RC elements under cyclic loading: State-of-the-art report.” Technical Report Bulletin d’information 230, COMITE EURO-INTERNATIONAL DU BETON, London, 1996.

[34] S. Brum and J. Fernando, “A model for the non linear dynamic analysis of reinforced concrete and masonry framed structures,” pp. 29–55, 2010.

[35] I. D. Karsan and J. O. Jirsan, “Behavior of Concrete Under Compressive Loadings,” *J. Struct. Devision*, vol. 95, no. ST12, pp. 2543–2563, 1969.

[36] B. P. Sinha, K. H. Gerstle, and L. G. Tulin, “Stress_strain Relations for Concrete under Cyclic Loading.” Journal of the ACI, 61(2), pp. 195–211, 1964.

[37] S.-Y. M. Ma, V. V. Bertero, and E. P. Popov, “Experimental and Analytical Studies of the Hysteretic Behavior of Reinforced Concrete Rectangular and T-beams.” Report EERC-76-2. EERC, University of California, Berkeley, 1976.

[38] J. Mander, M. Priestley, and R. Park, “Seismic design of bridge piers.” Research Report 84-2. Department of Civil Engineering, University of Canterbury, Christchurch, New Zealand, 1984.

[39] L. Dodd and J. Restrepo-Posada, “Model for predicting cyclic behavior of reinforcing steel,” *J. Struct. Eng.*, vol. 121, no. 3, pp. 433–445, 1995.

[40] F. C. Filippou, E. P. Popov, and V. V. Bertero, “Effect of Bond Deterioration on Hysteretic Behavior of Reinforced Concrete Joints.” p. 212, 1983.

[41] M. Papia, G. Russo, and G. Zingone, “Instability of longitudinal bars in RC columns,” *J. Struct. Eng. ASCE*, vol. 114, no. 2, pp. 445–461, 1988.

[42] B. S. T. Mau and M. El-mabsout, “Inelastic buckling o f reinforcing bars,” vol. 115, no. 1, pp. 1–17, 1989.

[43] S. Watson, F. A. Zahn, and R. Park, “Confining Reinforcement for Concrete Columns,” *Journal of Structural Engineering*, vol. 120, no. 6. pp. 1798–1824, 1994.

[44] G. Monti and C. Nuti, “Nonlinear Cyclic Behavior of Reinforcing Bars Including Buckling,” *J. Struct. Eng.*, vol. 118, no. 12, pp. 3268–3284, 1992.

[45] S. J. Pantazopoulou, “Detailing for Reinforcement Stability in RC Members,” *Journal of Structural Engineering*, vol. 124, no. 6. pp. 623–632, 1998.

[46] S. H. Suda K, Murayama Y, Ichinomiya T, “Buckling behavior of longitudinal reinforcing bars in concrete column subjected to reverse lateral loading.” Proceedings of the 11th World Conference on Earthquake Engineering 1996, CD ROM Paper No. 1753.

[47] M. E. Rodriguez, J. C. Botero, and J. Villa, “Cyclic Stress-Strain Behavior of Reinforcing Steel Including Effect of Buckling,” *Journal of Structural Engineering*, vol. 125, no. 6. pp. 605–612, 1999.

[48] R. P. Dhakal and K. Maekawa, “Path-dependent cyclic stress-strain relationship of reinforcing bar including buckling,” *Eng. Struct.*, vol. 24, no. 11, pp. 1383–1396, 2002.

[49] M. S. Hoehler and J. F. Stanton, “Simple Phenomenological Model for Reinforcing Steel under Arbitrary Load,” *J. Struct. Eng.*, vol. 132, no. 7, pp. 1061–1069, 2006.

[50] Giuffre; A. and Pinto; P. E., “II Comportamento Del Cemento Armato Per Sollecitazioni Cicliche di Forte Intensita,” *G. del Genio Civile, Maggio*, 1970.

[51] M. Menegotto and P. E. Pinto, “Method of Analysis for Cyclically Loaded R. C. Plane Frames Including Changes in Geometry and Non-Elastic Behavior of Elements under Combined Normal Force and Bending,” *Proc. IABSE Symp. Resist. Ultim. Deform. Struct. Acted by Well Defin. Loads*, pp. 15–22, 1973.

[52] V. Petrangeli, M. and Ciampi, “A flexibility based 3-dimensional fibre beam element.” Proceedings of Eight Italian Conference on Computational Mechanics, Torino, Italy, 1994.

[53] P. KOTRONIS∗ and J. MAZARS, “SIMPLIFIED MODELLING STRATEGIES TO SIMULATE THE DYNAMIC BEHAVIOUR OF R/C WALLS,” *Journal of Earthquake Engineering*, vol. 9, no. 2. pp. 285–306, 2005.

[54] E. Filippou, F. C. and Spacone, “FEDEAS: Nonlinear Analysis for Structural Evaluation.” Proceedings of the Eleventh Word Conference on Earthquake Engineering, Mexico., 1996.

[55] R. L. Taylor, “A finite element analysis program, Version 7.3.” Manual, University of California, Berkeley, California, 2000.

[56] D. Ferreira, A. Marí, and R. Faria, “A model for the nonlinear, time-dependent and strengthening analysis of shear critical frame concrete structures,” no. February, 2013.

[57] D. C. S. Ferreira, “Computer Program CONSHEAR Nonlinear analysis of concrete structures critical to shear,” no. April, 2013.

[58] I. P. Zararis, M. K. Karaveziroglou, and P. D. Zararis, “Shear Strength of Reinforced Concrete T-Beams,” no. 103, 2007.

[59] O. C. Zienkiewicz and R. L. Taylor, *The Finite Element Method Volume 1 : The Basis*, vol. 1. 2000.

[60] F. J. Vecchio and M. P. Collins, “PREDICTING THE RESPONSE OF REINFORCED CONCRETE BEAMS SUBJECTED TO SHEAR USING MODIFIED COMPRESSION FIELD THEORY.,” *ACI Struct. J.*, vol. 85, no. 3, pp. 258–268, 1988.

[61] M. A. Crisfield, “Non-Linear Finite Element Analysis of Solids and Structures.” Vol. 1 Essentials, John Wiley & Sons, West Sussex, 1996.

[62] R. P. Dhakal and K. Maekawa, “Modeling for Postyield Buckling of Reinforcement,” *J. Struct. Eng.*, vol. 128, no. 9, pp. 1139–1147, 2002.

[63] P. P. E. E. R. Center., “http://nisee.berkeley.edu/spd/servlet/display?format=html&id=199.” .

Annex A

The VBA code of the algorithm presented in Chapter 4.3.

```
Sub Steel()

 'all material constant input
    'input tension
    fy = Range("G6").Value
    fu = Range("G7").Value
    fsh1 = Range("G19").Value
    eps_y = Range("G10").Value
    eps_sh = Range("G11").Value
    eps_u = Range("G12").Value
    eps_sh1 = Range("G20").Value
    E0 = Range("G2").Value

    'input compression
    fyn = -Range("G6").Value
    fun = -Range("G7").Value
    eps_yn = -Range("G10").Value
    eps_shn = -Range("G11").Value
    eps_un = -Range("G12").Value

    'input coeficients
    R0 = 20
    a1 = 18.5
    a2 = 0.15 '0.05-0.15

    'input buckling
     L = Range("G15").Value
     D = Range("G16").Value

'Input variables:
     ratio = Range("R9")
     eps_I = Range("R10")
     fi = Range("R11")
     buckling = Range("R2")

    'input deformation
    eps_old = Round(Range("N2").Value, 5)     '(eps)
    sigma_old = Range("N3").Value       '(sigma)
    E_old = Range("N4").Value          '(E)
    increment = Round(Range("K3").Value, 5)
```

```
'input cyclic loops
  r = Range("K8")
  b = Range("K9")

'input intersection points
    eps_int = Range("R12")
    sig_int = Range("R13")

'input variables
    eps_R_max = Range("N6").Value
    eps_R_poz = Range("N7").Value
    sig_R_poz = Range("N8").Value
    sig_R_max = Range("N9").Value
    sig_R_max_envelope = Range("N10").Value
    E1_poz = Range("N11").Value
    E0_poz = Range("N12").Value

    eps_R_min = Range("N14").Value
    eps_R_neg = Range("N15").Value
    sig_R_neg = Range("N16").Value
    sig_R_min = Range("N17").Value
    sig_R_min_envelope = Range("N18").Value
    E1_neg = Range("N19").Value
    E0_neg = Range("N20").Value


    'variables to follow path:
        i = Range("R3")
        j = Range("R4")
        k = Range("R5")

    'intput for error poz side
        'error_poz
        error_poz = Range("R7")


    'calculate new eps
    eps = Round(eps_old + increment, 5)
```

```
 If (buckling = 0) Then
'Calculus for buckling point
   'calculate eps_i and ratio=fi/fit
     eps_I = eps_yn * (55 - 2.3 * Sqr(fy / 100) * L / D)
     If (eps_I / eps_yn < 7) Then
          eps_I = eps_yn * 7
     End If
  'calculate alpha
     alpha = 0.75 + (eps_u - eps_sh) / (300 * eps_y)
        If alpha > fu / (1.5 * fy) Then
        alpha = fu / (1.5 * fy)
          If alpha < 0.75 Then
            alpha = 0.75
          ElseIf alph + a > 1 Then
            alpha = 1
          End If
        End If

  'find fit and ratio=fi/fit
    If ((-eps_I) <= eps_sh) Then
         fit = fyn
         fi = fit * alpha * (1.1 - 0.016 * Sqr(fy / 100) * (L / D))
               If fi / fyn < 0.2 Then
                  fi = 0.2 * fyn
               End If
         ratio = fi / fit
      ElseIf ((-eps_I) <= eps_u) Then
         P = Log((fu - fsh1) / (fu - fy)) / Log((eps_u - eps_sh1) / (eps_u - eps_sh))
         fit = -(fu + (fy - fu) * ((eps_u - (-eps_I)) / (eps_u - eps_sh)) ^ P)
         fi = fit * alpha * (1.1 - 0.016 * Sqr(fy / 100) * (L / D))
               If fi / fyn < 0.2 Then
                  fi = 0.2 * fyn
               End If
         ratio = fi / fit
      Else
         ratio = 1
     End If
   buckling = 1
   End If
```

```
If (i = 0) Then
      If (eps >= 0) Then
          'tension
        If (eps <= eps_y) Then
          sigma = E0 * eps
          E = E0

        ElseIf (increment > 0) Then
          If (eps <= eps_sh) Then
            sigma = fy
            E = 0.1

          ElseIf (eps <= eps_u) Then
            P = Log((fu - fsh1) / (fu - fy)) / Log((eps_u - eps_sh1) / (eps_u - eps_sh))
            sigma = fu + (fy - fu) * ((eps_u - eps) / (eps_u - eps_sh)) ^ P
            E = ((fy - fu) / (eps_u - eps_sh) ^ P) * P * (eps_u - eps) ^ (P - 1) * (-1)

              'to be sure E isn't 0
              If E < 0.1 Then
                E = 0.1
              End If
          ElseIf (eps > eps_u) Then
            i = 3
          End If
        Else: i = 1
        End If

      Else
          'Compression
        If (eps >= eps_yn) Then
          sigma = E0 * eps
          E = E0
        ElseIf (increment < 0) Then
          If (eps >= eps_I) Then
            'find sigma_t
              If ((-eps) <= eps_sh) Then
                sig_t = fyn
              ElseIf ((-eps) <= eps_u) Then
                P = Log((fu - fsh1) / (fu - fy)) / Log((eps_u - eps_sh1) / (eps_u - eps_sh))
                sig_t = -(fu + (fy - fu) * ((eps_u - (-eps)) / (eps_u - eps_sh)) ^ P)
              ElseIf ((-eps) > eps_u) Then
              i = 3
              End If
            If (i < 3) Then
            sigma = sig_t * (1 - (1 - ratio) * ((eps - eps_y) / (eps_I - eps_y)))
            'calculate E
              If ((-eps) <= eps_sh) Then
```

```
                    E = (-1) * sig_t * (1 - ratio) * (1 / (eps_I - eps_y))
                ElseIf ((-eps) <= eps_u) Then
                    E = ((1) * ((fy - fu) / (eps_u - eps_sh) ^ P) * P * (eps_u - (-eps)) ^ (P - 1) * (-1)) +
((-1) * (((fy - fu) / (eps_u - eps_sh) ^ P) * P * (eps_u - (-eps)) ^ (P - 1) * (-1)) * ((1 - ratio) * ((eps - eps_y)
/ (eps_I - eps_y)))) + ((1) * (fu + (fy - fu) * ((eps_u - (-eps)) / (eps_u - eps_sh)) ^ P)) * ((1 - ratio) * (1 /
(eps_I - eps_y)))
                End If
                    'limit E
                    If (E < (-0.03 * E0)) Then
                        E = -0.03 * E0
                    End If
                    If (E < 0.1 And E > -0.1) Then
                        E = 0.1
                    End If
              Else: End If
            ElseIf (eps >= eps_un) Then
                sigma = fi - 0.02 * E0 * (eps - eps_I)
                    If (sigma / fyn <= 0.2) Then
                        sigma = 0.2 * fyn
                    End If
                E = -0.02 * E0
            ElseIf (eps < eps_un) Then
              i = 3
            End If
          Else: i = 1
        End If
      End If
End If


If (i = 1) Then
 'initialize at the exit from elastic
   If increment < 0 Then
      eps_R_max = eps_old
      eps_R_poz = eps_old
      sig_R_poz = sigma_old
      sig_R_max = sigma_old
      sig_R_max_envelope = sigma_old
      E1_poz = E_old
      E0_poz = E0 * (0.82 + 1 / (5.55 + 1000 * eps_R_max))

      eps_R_min = eps_yn
      eps_R_neg = eps_yn
      sig_R_neg = fyn
      sig_R_min = fyn
      sig_R_min_envelope = fyn
      E1_neg = (-1) * fyn * (1 - ratio) * (1 / (eps_I - eps_y))
```

```
            If (E1_neg < 0.1) Then
                E1_neg = 0.1
            End If
        E0_neg = E0
        i = 2
    Else
        eps_R_min = eps_old
        eps_R_neg = eps_old
        sig_R_neg = sigma_old
        sig_R_min = sigma_old
        sig_R_min_envelope = sigma_old
        E1_neg = E_old
            'limit E1_neg
              If (E1_neg <= 0) Then
                 E1_neg = 0.1
              End If
             'find sigma_t
              If ((-eps_old) <= eps_sh) Then
                  sig_t = fyn
              ElseIf ((-eps_old) <= eps_u) Then
                  P = Log((fu - fsh1) / (fu - fy)) / Log((eps_u - eps_sh1) / (eps_u - eps_sh))
                  sig_t = -(fu + (fy - fu) * ((eps_u - (-eps_old)) / (eps_u - eps_sh)) ^ P)
              End If
        E0_neg = E0 * (sig_R_neg / sig_t) ^ 2
        eps_R_max = eps_y
        eps_R_poz = eps_y
        sig_R_poz = fy
        sig_R_max = fy
        sig_R_max_envelope = fy
        E1_poz = 0.1
        E0_poz = E0
        i = 2

    End If
End If
```

```
If (i = 2) Then

    'unload from tension curve
    If increment < 0 Then

        'condition when changing increment:
      If k = 1 Then

          'when exit load loop update conditions
            eps_R_poz = eps_old
            sig_R_poz = sigma_old

      ElseIf k = 2 Then
       'cond at return point for positive side
          If error_poz > 0 Then
                eps_R_poz = eps_old
                sig_R_poz = sigma_old
                eps_R_max = eps_old
                sig_R_max_envelope = fy
                error_poz = sig_R_max_envelope - sigma_old
                sig_R_max = sig_R_max_envelope + error_poz
                E1_poz = E_old
                E0_poz = E0 * (0.82 + 1 / (5.55 + 1000 * eps_R_max))
          Else
                eps_R_poz = eps_old
                sig_R_poz = sigma_old
                eps_R_max = eps_old
                sig_R_max_envelope = sigma_old
                sig_R_max = sigma_old
                E1_poz = E_old
                E0_poz = E0 * (0.82 + 1 / (5.55 + 1000 * eps_R_max))
          End If

       ElseIf k = 3 Then
        'cond at return point for positive side
          If error_poz > 0 Then
                eps_R_poz = eps_old
                sig_R_poz = sigma_old
                eps_R_max = eps_old
                P = Log((fu - fsh1) / (fu - fy)) / Log((eps_u - eps_sh1) / (eps_u - eps_sh))
                sig_R_max_envelope = fu + (fy - fu) * ((eps_u - eps_old) / (eps_u - eps_sh)) ^P
                error_poz = sig_R_max_envelope - sigma_old
                sig_R_max = sig_R_max_envelope + error_poz
                E1_poz = E_old
                E0_poz = E0 * (0.82 + 1 / (5.55 + 1000 * eps_R_max))
          Else
              eps_R_poz = eps_old
```

```
                    sig_R_poz = sigma_old
                    eps_R_max = eps_old
                    sig_R_max = sigma_old
                    sig_R_max_envelope = sigma_old
                    E1_poz = E_old
                    E0_poz = E0 * (0.82 + 1 / (5.55 + 1000 * eps_R_max))
                End If
            Else: End If
        k = 0

            If (j = 0) Then

            'calculate intersection point (ref.2)
             eps_int = (sig_R_min - sig_R_poz + E0_poz * eps_R_poz - E1_neg * eps_R_min) /
(E0_poz - E1_neg)
             sig_int = E0_poz * (eps_int - eps_R_poz) + sig_R_poz
             xi = Abs((eps_R_min - eps_int) / (eps_int - eps_R_poz))
             r = R0 - (a1 * xi) / (a2 + xi)
             b = E1_neg / E0_poz

                'check error
                eps_star = (eps_R_min - eps_R_poz) / (eps_int - eps_R_poz)
                sig_star = b * eps_star + ((1 - b) * eps_star) / ((1 + eps_star ^ r) ^ (1 / r))
                sig_R_min_witherror = sig_star * (sig_int - sig_R_poz) + sig_R_poz
                error_neg = sig_R_min_envelope - sig_R_min_witherror
                sig_R_min = sig_R_min + error_neg

                'calculate intersection point again
                eps_int = (sig_R_min - sig_R_poz + E0_poz * eps_R_poz - E1_neg * eps_R_min) /
(E0_poz - E1_neg)
                sig_int = E0_poz * (eps_int - eps_R_poz) + sig_R_poz
                xi = Abs((eps_R_min - eps_int) / (eps_int - eps_R_poz))
                r = R0 - (a1 * xi) / (a2 + xi)
                b = E1_neg / E0_poz
              j = 1
            End If


        If (eps >= eps_R_min) Then
            eps_star = (eps - eps_R_poz) / (eps_int - eps_R_poz)
            sig_star = b * eps_star + ((1 - b) * eps_star) / ((1 + eps_star ^ r) ^ (1 / r))
            sigma = sig_star * (sig_int - sig_R_poz) + sig_R_poz
            E = (sigma - sigma_old) / (eps - eps_old)
        Else 'enter on envelope
            'Compression
            If (eps >= eps_I) Then
                j = 2
```

```
                    'find sigma_t
                      If ((-eps) <= eps_sh) Then
                          sig_t = fyn
                      ElseIf ((-eps) <= eps_u) Then
                          P = Log((fu - fsh1) / (fu - fy)) / Log((eps_u - eps_sh1) / (eps_u - eps_sh))
                          sig_t = -(fu + (fy - fu) * ((eps_u - (-eps)) / (eps_u - eps_sh)) ^ P)
                      ElseIf ((-eps) > eps_u) Then
                          i = 3
                      End If
                    If (i < 3) Then
                     sigma = sig_t * (1 - (1 - ratio) * ((eps - eps_y) / (eps_I - eps_y)))
                      'calculate E
                      If ((-eps) <= eps_sh) Then
                          E = (-1) * sig_t * (1 - ratio) * (1 / (eps_I - eps_y))
                      ElseIf ((-eps) <= eps_u) Then
                          E = ((1) * ((fy - fu) / (eps_u - eps_sh) ^ P) * P * (eps_u - (-eps)) ^ (P - 1) * (-1)) +
((-1) * (((fy - fu) / (eps_u - eps_sh) ^ P) * P * (eps_u - (-eps)) ^ (P - 1) * (-1)) * ((1 - ratio) * ((eps - eps_y)
/ (eps_I - eps_y)))) + ((1) * (fu + (fy - fu) * ((eps_u - (-eps)) / (eps_u - eps_sh)) ^ P)) * ((1 - ratio) * (1 /
(eps_I - eps_y)))
                      End If
                          'limit E
                          If (E < (-0.03 * E0)) Then
                              E = -0.03 * E0
                          End If
                          If (E < 0.1 And E > -0.1) Then
                              E = 0.1
                          End If
                    Else: End If

                ElseIf (eps >= eps_un) Then
                      j = 3
                      sigma = fi - 0.02 * E0 * (eps - eps_I)
                           If (sigma / fyn <= 0.2) Then
                             sigma = 0.2 * fyn
                           End If
                      E = -0.02 * E0
                 ElseIf (eps < eps_un) Then
                   i = 3
                 End If
               End If
          End If
```

```
'unload from compression curve
If increment > 0 Then

        'condition when changing increment:
        If j = 1 Then
           'when exit load loop update conditions   j=1
              eps_R_neg = eps_old
              sig_R_neg = sigma_old

        ElseIf j = 2 Then

         'cond at return point for negative side (minimum conditions) j=2
            eps_R_neg = eps_old
            sig_R_neg = sigma_old
            eps_R_min = eps_old
            sig_R_min = sigma_old
            sig_R_min_envelope = sigma_old
            E1_neg = E_old
                  'limit E1_neg
                  If (E1_neg <= 0) Then
                  E1_neg = 0.1
                  End If
               'find sigma_t
               If ((-eps_old) <= eps_sh) Then
                  sig_t = fyn
               ElseIf ((-eps_old) <= eps_u) Then
                  P = Log((fu - fsh1) / (fu - fy)) / Log((eps_u - eps_sh1) / (eps_u - eps_sh))
                  sig_t = -(fu + (fy - fu) * ((eps_u - (-eps_old)) / (eps_u - eps_sh)) ^ P)
               End If
            E0_neg = E0 * (sig_R_min / sig_t) ^ 2
         ElseIf j = 3 Then

         'cond at return point for negative side j=3
            eps_R_neg = eps_old
            sig_R_neg = sigma_old
            eps_R_min = eps_old
            sig_R_min = sigma_old
            sig_R_min_envelope = sigma_old
            E1_neg = E_old
                  'limit E1_neg
                 If (E1_neg <= 0) Then
                 E1_neg = 0.1
                 End If
             'find sigma_t
               If ((-eps_old) <= eps_sh) Then
                  sig_t = fyn
               ElseIf ((-eps_old) <= eps_u) Then
```

```
                    P = Log((fu - fsh1) / (fu - fy)) / Log((eps_u - eps_sh1) / (eps_u - eps_sh))
                    sig_t = -(fu + (fy - fu) * ((eps_u - (-eps_old)) / (eps_u - eps_sh)) ^ P)
                End If
              E0_neg = E0 * (sig_R_min / sig_t) ^ 2
            Else: End If
          j = 0

          If k = 0 Then
          'calculate intersection point (ref.2)
          eps_int = (sig_R_max - sig_R_neg + E0_neg * eps_R_neg - E1_poz * eps_R_max) / (E0_neg
- E1_poz)
          sig_int = E0_neg * (eps_int - eps_R_neg) + sig_R_neg
          xi = Abs((eps_R_max - eps_int) / (eps_int - eps_R_neg))
          r = R0 - (a1 * xi) / (a2 + xi)
          b = E1_poz / E0_neg

             'check error
              eps_star = (eps_R_max - eps_R_neg) / (eps_int - eps_R_neg)
              sig_star = b * eps_star + ((1 - b) * eps_star) / ((1 + eps_star ^ r) ^ (1 / r))
              sig_R_max_witherror = sig_star * (sig_int - sig_R_neg) + sig_R_neg
              error_poz2 = sig_R_max_envelope - sig_R_max_witherror
              sig_R_max = sig_R_max + error_poz2

              'calculate intersection point again
              eps_int = (sig_R_max - sig_R_neg + E0_neg * eps_R_neg - E1_poz * eps_R_max) /
(E0_neg - E1_poz)
              sig_int = E0_neg * (eps_int - eps_R_neg) + sig_R_neg
              xi = Abs((eps_R_max - eps_int) / (eps_int - eps_R_neg))
              r = R0 - (a1 * xi) / (a2 + xi)
              b = E1_poz / E0_neg

            k = 1
          End If

          If (eps <= eps_R_max) Then

              eps_star = (eps - eps_R_neg) / (eps_int - eps_R_neg)
              sig_star = b * eps_star + ((1 - b) * eps_star) / ((1 + eps_star ^ r) ^ (1 / r))
              sigma = sig_star * (sig_int - sig_R_neg) + sig_R_neg
              E = (sigma - sigma_old) / (eps - eps_old)

                If (eps = eps_R_max) Then
                  If (eps <= eps_sh) Then
                      sig_envelope = fy
                      error_poz = sig_envelope - sigma

                   ElseIf (eps <= eps_u) Then
```

```
                P = Log((fu - fsh1) / (fu - fy)) / Log((eps_u - eps_sh1) / (eps_u - eps_sh))
                sig_envelope = fu + (fy - fu) * ((eps_u - eps) / (eps_u - eps_sh)) ^ P
                error_poz = sig_envelope - sigma
              End If
            End If

        Else   'enter on envelope

          If (eps <= eps_sh) Then
            k = 2

             error_poz = error_poz - error_poz * increment / (5 * eps_y)

              If error_poz > 0 Then
                sigma = fy - error_poz
                E = 0.1
              Else
                sigma = fy
                E = 0.1
              End If

           ElseIf (eps <= eps_u) Then
             k = 3
             error_poz = error_poz - error_poz * increment / (5 * eps_y)
                 If error_poz > 0 Then
                   P = Log((fu - fsh1) / (fu - fy)) / Log((eps_u - eps_sh1) / (eps_u - eps_sh))
                   sigma = fu + (fy - fu) * ((eps_u - eps) / (eps_u - eps_sh)) ^ P - error_poz
                   E = ((fy - fu) / (eps_u - eps_sh) ^ P) * P * (eps_u - eps) ^ (P - 1) * (-1)
                        'to be sure E isn't 0
                        If E < 0.1 Then
                          E = 0.1
                        End If
                 Else
                   P = Log((fu - fsh1) / (fu - fy)) / Log((eps_u - eps_sh1) / (eps_u - eps_sh))
                   sigma = fu + (fy - fu) * ((eps_u - eps) / (eps_u - eps_sh)) ^ P
                   E = ((fy - fu) / (eps_u - eps_sh) ^ P) * P * (eps_u - eps) ^ (P - 1) * (-1)
                       'to be sure E isn't 0
                        If E < 0.1 Then
                            E = 0.1
                        End If
                 End If
            ElseIf (eps > eps_u) Then
              i = 3
            End If
          End If
      End If
End If
```

```
'output:
'output pricincipal info
    Range("N2") = eps
    Range("N3") = sigma
    Range("N4") = E

'output path track variable
Range("R3") = i
 Range("R4") = j
 Range("R5") = k

'output buckling
Range("R9") = ratio
 Range("R10") = eps_I
 Range("R2") = buckling
 Range("R11") = fi

 'output for error poz side
Range("R7") = error_poz

'output variables
   Range("N6").Value = eps_R_max
   Range("N7").Value = eps_R_poz
   Range("N8").Value = sig_R_poz
   Range("N9").Value = sig_R_max
   Range("N10").Value = sig_R_max_envelope
   Range("N11").Value = E1_poz
   Range("N12").Value = E0_poz

   Range("N14").Value = eps_R_min
   Range("N15").Value = eps_R_neg
   Range("N16").Value = sig_R_neg
   Range("N17").Value = sig_R_min
   Range("N18").Value = sig_R_min_envelope
   Range("N19").Value = E1_neg
   Range("N20").Value = E0_neg
'output cyclic loop
Range("K8") = r
Range("K9") = b

'output intersection points
   'eps_int
   'sig_int
   Range("R12") = eps_int
   Range("R13") = sig_int

End Sub
```